Environmental Science and Pollution Research (2018) 25:25840–25861
https://doi.org/10.1007/s11356-018-2767-7

REVIEW ARTICLE

Three-dimensional graphene-based adsorbents in sewage disposal: a review

Lei Chen[1] · Qiaoqiao Han[1] · Wenxiao Li[1] · Zhiyong Zhou[1] · Zhou Fang[1] · Zhiwei Xu[1] · Zexiang Wang[2] · Xiaoming Qian[1]

Received: 6 May 2018 / Accepted: 13 July 2018 / Published online: 23 July 2018

Abstract

A kind of graphene functional materials based on three-dimensional (3D) porous structure is a new star for environmental application in the past decades because it not only inherits the perfect carbon crystal structure of two-dimensional (2D) graphene sheets but also exhibits several advantages such as extremely low density, high porosity, and big surface area, all which enable diverse contaminants to easily access and diffuse into 3D networks, and make these materials ideal adsorbents with superior adsorptivity and recyclability. This review aims to summarize the recent progress in constructing 3D graphene-based adsorbents (3DGBAs) with two hybrid systems such as graphene/polymers and graphene/inorganic nanomaterials, and to provide a fundamental understanding of synthetic methods for interconnecting these nanostructures, structure–property relationships, and extensive applications in environmental protection towards adsorption of heavy metals, dyes, oils, and organic pollutants. Furthermore, we make a forecast on the future development opportunities and technical challenges, which is hoped to make an inspiration for the researchers to exploit a new family of graphene-based adsorption materials.

Keywords Three-dimensional graphene · Polymers · Inorganic nanomaterials · Adsorption · Pollutants

Introduction

Water is a necessary resource, which has a great effect on the world's economic, social, and environment conditions. As the control ways of contamination are lagging behind the rapid economic development, water pollution and associated environmental issues turn into a very tough problem, which has received a wide range of global attention. In the last few decades, magnanimous efforts have been made to research the various materials in order to adsorb and mitigate water pollutants, in which three-dimensional (3D) porous materials possess substantial advantages such as controllable pores and voids and play a particularly important role in environmental protection (Gokulakrishnan et al. 2007; Kemp et al. 2013; Kondo et al. 2007). Of these, more attention has been paid to the carbon-based nanomaterials (Shi et al. 2016a; Wang et al. 2018b; Wu et al. 2018), especially the 3D porous graphene hybrid systems (Liu et al. 2012; Shi et al. 2016b; Tan et al. 2015).

Graphene, a honeycomb-like single-layer reticular two-dimensional (2D) crystal connected by sp^2 hybridized carbon atoms, has attracted tremendous attention due to its excellent physical and chemical properties, such as great ultimate strength (125 GPa) and huge specific surface area (2630 $m^2\ g^{-1}$) (Bolotin et al. 2008; Frank et al. 2007). Nevertheless, graphene sheets have a tendency to produce irreversibly agglomerate and re-stacking as a result of strong π–π bonds and van der Waals forces, which leads to available specific surface area of graphene material far below the theoretical value and restricts them in practical utilization to a great extent (Li et al. 2008). How to efficiently exploit the exceptional properties of graphene became a significant opportunity and challenge for researchers around the world. To prevent the abovementioned phenomenon, assembling 2D graphene sheets into 3D macroscopic structures have been

Responsible editor: Philippe Garrigues

✉ Lei Chen
chenlei@tjpu.edu.cn

[1] Key Laboratory of Advanced Braided Composites, Ministry of Education, School of Textiles, Tianjin Polytechnic University, Tianjin 300160, People's Republic of China

[2] Tianjin Xuwo Technology Co., Ltd., Tianjin 300000, People's Republic of China

recognized as one of the most promising strategies because of a primary aspect that it allows the resulting 3D graphene materials not only to retain the inherently outstanding properties of individual graphene sheets but also to further develop collective advantageous properties such as remarkable electronic and mechanical properties, low density, and high porosity (Papandrea et al. 2016; Xu et al. 2015). Besides, our team has also made a great deal of effort in construction of 3D graphene composites (Gao et al. 2016; Ni et al. 2015; Wang et al. 2018a; Zhu et al. 2016b), and their application of adsorption contaminants from water (Xu et al. 2014). Due to the internal connection framework and well-defined porous structure of these 3D networks, the 3DGBAs are provided with accessibility of the internal surface area and facile mass transport, which offers an extremely excellent candidate for disposal and adsorption of various contaminants linking up with their remarkably inherent properties such as hydrophobicity and mechanical stability (Liu et al. 2012). In addition, another significant ascendency is that the integrated morphology of 3D graphene networks makes it convenient for manipulation and collection during the use in water environment, which defends the release of graphene sheets and reduces the damage to the aquatic environment (Zhao et al. 2014).

The numerous functional application capabilities of 3D graphene materials are difficult to further extend if macroscopic frameworks merely rely on weak electrostatic interaction and hydrogen or π–π bonds in nature between the graphene sheets. Therefore, it is desperately urgent to inject late-model functional components into the basis of the 3D graphene networks served to manipulate these forces by changing them the chemical environment. Recently, according to the application needs, researchers have designed and constructed substantial 3D graphene-based composites with various frameworks (hydrogels (Bai et al. 2010; Tiwari et al. 2013), aerogels (Hu et al. 2013a; Ye et al. 2013; Zhu et al. 2015), sponges (Bi et al. 2012; Zhang et al. 2014a), and foams (Yavari et al. 2011)) and different functional components (polymers (Chen et al. 2013b; Gao et al. 2013), metallic (Singh et al. 2013; Zhang et al. 2013c) and non-metallic nanomaterials (Kabiri et al. 2014; Wan et al. 2016)) through abundant physical and chemical pathways, such as cross-linking method and reduction self-assembly method. Although there have been a modicum of reviews about synthesis approaches and environmental protect application of 3D graphene-based composites in the past (Ma and Chen 2015; Rethinasabapathy et al. 2017; Riaz et al. 2017; Shen et al. 2015; Zeng et al. 2013; Zhou et al. 2014), we find that a systematical and comprehensive summary of 3DGBAs about two hybrid systems of graphene/polymers and graphene/inorganic nanomaterials continues to be blank. The high-speed development of this field convinces us that 3DGBAs will be the new generation of materials in sewage disposal and environmental protection due to controllable structure and extraordinary adsorption performance. Thus, the review is intended to systematically summarize the environment applications of these two 3DGBA systems, mainly concentrating on the preparation methods and adsorption mechanism of 3DGBAs for various types of contaminants.

Herein, the preceding part of this review summarizes the building methods of these two 3DGBA systems. The construction mechanisms and the structure–property relationships are also elaborated in detail. The latter part systematically presents potential applications of a diversity of 3DGBAs in water environmental pollutant removal, such as heavy metal ions, dyes, oils, and organic pollutants. The performances and the adsorption mechanisms of them are compared with each other in several tables. Finally, we also briefly sum up the current difficulties faced in the assembling and application as well as shed light on future prospects.

Assembling of 3D graphene/polymer adsorbents

Introducing polymer with graphene to fabricate 3D graphene/polymers adsorbents shows fascinating prospects due to the obviously synergistic effect. In most cases, the synthetic strategies of these adsorbents commonly start from graphene oxide (GO) because chemical inertness of graphene hinders its controllability of assembling into 3D architectures (Bai et al. 2011) and can be roughly split into three categories, including cross-linking methods, reduction self-assembly methods, and others. All of the strategies lead to 3DGBAs with diverse morphologies, microstructures, and properties. These approaches and the structures of the corresponding 3D graphene/polymer adsorbents will be discussed in the following subsections in detail. Table 1 gives a systematic comparison of the preparation procedure for a diversity of 3D graphene/polymer adsorbents.

Cross-linking methods

GO sheets, densely decorated with various hydrophilic oxygenated functional groups (epoxy, carboxyl, and hydroxyl groups), can be readily dispersed in numerous solvents (Chen et al. 2017; Li et al. 2008). Hence, integrating GO sheets and polymers with the presence of cross-linkers in aqueous or organic media could successfully realize construction of 3DGBAs, in which the formation of resulting adsorbents mainly rely on covalent bonds and noncovalent bonds (electrostatic interaction, hydroxyl bonding, and π–π stacking) (Dizaji et al. 2016). With a typical example of covalent bonds, Luo et al. successfully produced the 3D poly3-aminopropyltriethoxysilane oligomeric (PAS)-GO porous composites to adsorb heavy metal ions (Pb^{2+}) (Luo et al. 2014). The construction of 3D network exploited covalent

Table 1 The preparation procedure for a diversity of 3D graphene/polymer adsorbents

Strategies	Original carbon materials	Monomer/polymers	Other agent	Required maximum temperature (°C)	Process difficulties	Adsorption capacity	Reference
Cross-linking methods	Graphene oxide	3-aminopropyltriethoxysilane	Ethanol	Room temperature	Easy	Pb^{2+} (312.5 mg g^{-1})	(Luo et al. 2014)
	Graphene oxide	Polyvinyl alcohol	Saturated Na_2SO_4	95	Easy	MB (476.2 mg g^{-1})	(Yang et al. 2016)
	Graphene oxide	Carboxymethyl cellulose sodium	Citric acid	60	Easy	MB (59 mg g^{-1}) and eosin Y (66 mg g^{-1})	(Liu et al. 2016a)
	Graphene oxide	Anionic polyacrylamide	–	Room temperature	Easy	Basic fuchsin (1034.3 mg g^{-1})	(Yang et al. 2015a)
	Graphene oxide	Polyethylenimine	Cetyl trimethylammonium bromide	Room temperature	Easy	Amaranth (800 mg g^{-1})	(Sui et al. 2013)
	Graphene oxide	Polyvinyl alcohol, chitosan	$CaCl_2$-saturated boric acid solution	100	Easy	Cu^{2+} (162 mg g^{-1})	(Li et al. 2015)
	Graphene oxide	Poly(acrylic acid)	Hydrogen iodide vapor	Room temperature	Easy	Oil (120 g g^{-1})	(Ha et al. 2015)
Reduction self-assembly methods	Graphene oxide	Poly(acrylic acid)	Ar atmosphere	800	Easy	MB (1050 mg g^{-1})	(Tao et al. 2014)
	Graphene oxide	Dopamine	–	60	Easy	Pb^{2+} (336.32 mg g^{-1})	(Gao et al. 2013)
	Graphene oxide	Gelatin	–	90	Easy	RB (280.8 mg g^{-1})	(Liu et al. 2017a)
	Graphene oxide	β-Cyclodextrin, chitosan	Sodium ascorbate	90	Easy	MB (1134 mg g^{-1})	(Liu et al. 2018)
	Graphene oxide	Cotton linter	Methanol, sodium azide, *p*-toluenesulfonyl chloride, dimethylformamide, pyridine	110	Hard	MB (122.5 mg g^{-1})	(Soleimani et al. 2018)
	Graphene oxide	Dopamine, chitosan	Glutaraldehyde, 1H,1H,2H,2H-perfluorodecanethiol, methanol	180	Hard	Ethanol (~ 20 g g^{-1})	(Cao et al. 2017)
Other methods	Graphene oxide	Commercial polyurethane foam	Diphenyl-methane-diisocyanate, polyether polyols, nano-$CaCO_3$, 1,4-diazabicyclo(2.2.2)octane, stannous octoate, polydimethylsiloxane, ethylene diamine	90	Hard	Quickly and selectively absorbed the toluene from the mixture	(Zhu et al. 2016a)
	Graphene oxide	2-Acrylamido-2-methylpropane sulfonic acid, acrylamide, starch	*N*,*N*′-Methylenebisacrylamide, calcium carbonate, ammonium persulfate	70	Hard	MB (714.29 mg g^{-1})	(Pourjavadi et al. 2016)
	Reduced graphene oxide	Polycarbonate pellets	Tetrahydrofuran	40	Easy	CCl_4 (17.57 g g^{-1})	(Wang et al. 2018b)
	Graphene oxide	Sodium alginate powder	Calcium chloride, vitamin C	80	Easy	Phenol (49.358 mg g^{-1})	(Feng et al. 2017)

cross-linking between epoxy groups on GO sheets and a great quantity of amino groups of PAS. What needs to be mentioned is that noncovalent interactions are frequently and extensively exploited to construct 3D adsorbents on account of the damage free to inherent structure of graphene. Tremendous work has been done to investigate the integrating GO sheets and polymers triggered by the hydrogen bonding. For instance, polyvinyl alcohol (PVA) (Li et al. 2014a; Ma 2016; Wang et al. 2014a; Yang et al. 2016) and carboxymethyl cellulose sodium (CMCNa) (Liu et al. 2016a) have been successfully introduced into GO sheet for preparing 3DGBAs via hydrogen bonding. Typically, Liu's group fabricated the CMCNa/GO hydrogel microparticles (CGs) by mixing the CMCNa solution and GO suspension and spray drying methods, and the cross-linking network can be effectively formed by hydrogen bonding (see Fig. 1), and the obtained CGs showed the excellent adsorption effect to methylene blue (MB), eosin, and various heavy metals (Liu et al. 2016a). In addition, electrostatic interaction is another key driver for assembly of GO sheets into 3D network architectures with polymers. GO sheets, with negative electric charges because of the ionization of oxygen-containing surface groups, could be the desirable material for forming cross-linking networks with positively charged polymers via electrical reaction. There are now a great deal of polymers, such as polyacrylamide (PAM) (Hosseinzadeh and Ramin 2017; Qi et al. 2015; Ren et al. 2010; Yang et al. 2015a, 2017a, d) and polyethylenimine (PEI) (Sui et al. 2013; Wang et al. 2017c), have been successfully introduced into GO sheets to induce the assembly of 3D porous structures through electrostatic interaction. As an important example, Yang et al. proposed a mechanism for preparation of 3D GO/PAM composite hydrogels, and the cross-linking network was the result of strong attractions between the carboxyl groups of GO sheets and amine groups of PAM chains (Yang et al. 2017d). To further improve the adsorption properties of 3DGBAs, two or more kinds of polymers have also been inserted into GO sheets to form 3D porous and multicomponent network (Li et al. 2015; Yang et al. 2017b). For instance, the PVA/CS/GO hydrogel beads were prepared by an instantaneous gelation method, and the adsorbents exhibited high removal efficiency of Cu^{2+} from aqueous solutions compared with PVA/CS adsorbents (Li et al. 2015).

In some case, 3DGBAs require the superhydrophobicity and superlipophilicity, such as the oil–water separation. So it is necessary to further convert 3D GO/polymer materials into 3D reduced graphene oxide (rGO)/polymer materials with the aid of some reduction techniques. For a typical example, Ha et al. prepared the poly(acrylic acid) (PAA)/rGO aerogels with high porosity (> 99%), low density (~ 3–10 mg cm^{-3}), excellent mechanical property (can support up to 10,000 times their weight), and outstanding oil adsorption capacities (~ 120 g g^{-1}) (Ha et al. 2015). The detail preparation process is shown in Fig. 2. Due to hydrogen bonding or covalent interactions, PAAs appeared to form a stringy, dendritic structure positioned on the rGO surface and in the pores after thermal cross-linking and reducing GO, which was beneficial for the enhancement in the overall stiffness and robustness of aerogels.

Reduction self-assembly methods

The reduction self-assembly has been considered as one of the most simple, effective, and attractive methods for preparing

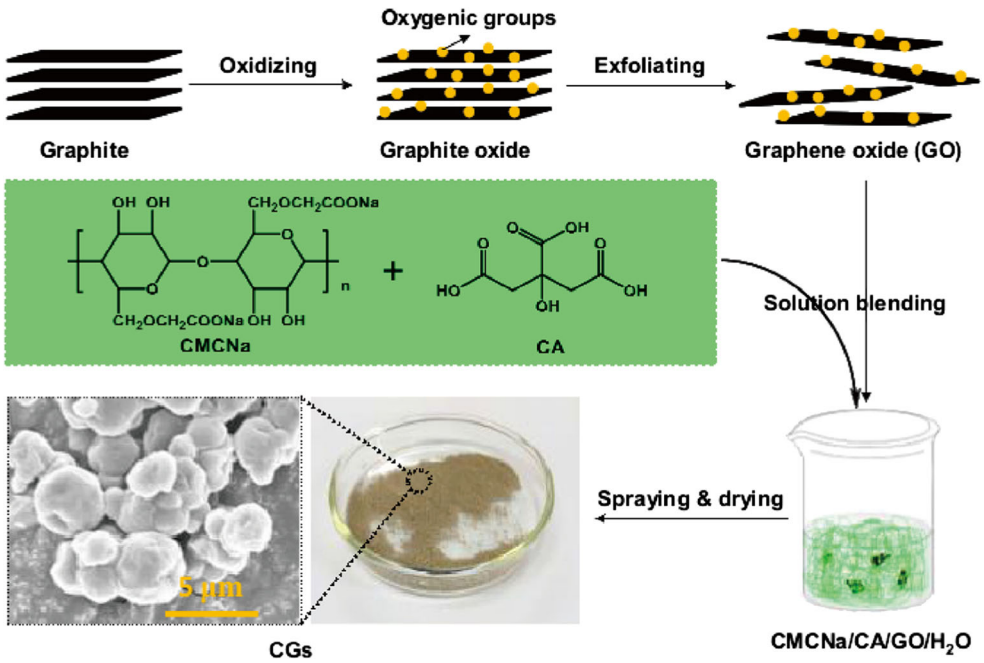

Fig. 1 Schematic illustration for the fabrication process of CGs (Liu et al. 2016a)

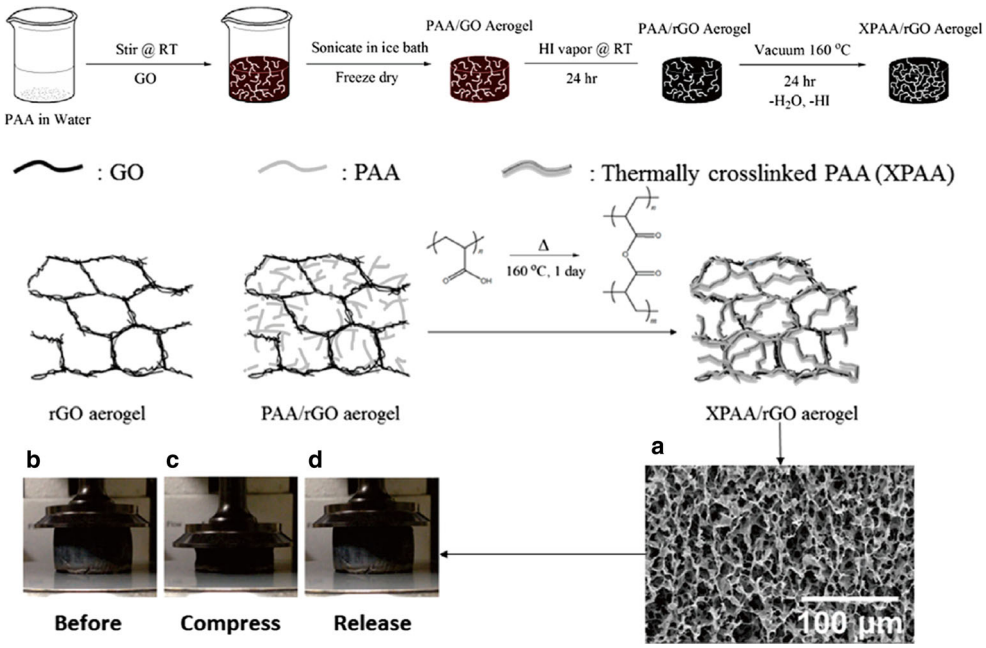

Fig. 2 Schematic illustration for the fabrication process of XPAA/rGO aerogels: SEM (**a**) and digital images showing the compressibility of 450 kDa/50 during the 10th compression/release cycle (**b**–**d**) (Ha et al. 2015)

3D graphene/polymers composites because the inserted polymers during the reduction self-assembly process play the role of spacers to further restrain the agglomerate and re-stacking of rGO, which is different from other preparation routes (Huang et al. 2014; Xiao et al. 2017). In this approach, the 3D interconnected porous networks are generally prepared by mixing the GO with polymers or its precursor to achieve a stable and uniform dispersion solution and then directly assembling them during the reduction GO process. The formation of the 3D composites is mainly driven by the synergistic reaction of the partial π–π stacking interaction, hydrogen bonding, electrostatic interaction, and increased van der Waals forces caused by reduction of GO. For instance, Tao's group constructed 3D reduced expanded porous graphene macroform (r-EPGM) through hydrothermal self-assembly of GO sheets with PVA as linker (Tao et al. 2014). The procedure schematic and morphology pictures are shown in Fig. 3. The introduced linear chains of PVA can bridge GO sheets to form a more expanded structure by hydrogen bonding, which effectively facilitated the intercalation of polymers and curbed the agglomerate and re-stacking of rGO.

Moreover, it is worth noting that there are various biopolymers that have already been anchored successfully into rGO sheets to construct 3DGBAs during the process of reducing GO, such as polydopamine (PDA) (Gao et al. 2013; Wang et al. 2014b), chitosan (CS) (Guo et al. 2016; Liu et al. 2018), gelatin (Liu et al. 2017a), cellulose (Soleimani et al. 2018), and lignosulfonate (Li et al. 2016a). Typically, 3D PDA-modified graphene hydrogel (PDA-GH) can be synthesized via one-step approach, in which dopamine acted as reductant and surface functionalization agents (Gao et al. 2013). The PDA-GH was synthesized by directly mixing the GO aqueous solution and dopamine solution and then the mixture was heated at 60 °C for 6 h. The prepared adsorbents exhibited excellent adsorption performances to a wide spectrum of pollutions, such as heavy metal ions (Pb^{2+} and Cd^{2+}), cationic dyes (rhodamine B (RhB) and *p*-nitrophenol), and aromatic contaminants. Besides, Liu's group fabricated a 3D reduced graphene oxide aerogel (GRGO) by the in situ reducing assembly of GO sheets with using gelatin as the reducing agent and cross-linker (Liu et al. 2017a). The synthetic process is illustrated in Fig. 4a. The GRGO aerogels showed outstanding adsorption capacities to cationic organic dyes (RhB (280.8 mg g^{-1}), MB, crystal violet (CV)), and the adsorption efficiencies at 303 K toward RhB, MB, CV, and neutral red (NR) were 95.8%, 92.1%, 79.1%, and 70.5%, respectively. Additionally, reduction self-assembly has also been used to prepare multicomponent 3DGBAs. For example, a 3D β-cyclodextrin/CS functionalized GO hydrogel was prepared by reduction method with the sodium ascorbate served as reducing agent, and the resulting products had excellent adsorption capacity toward MB (1134 mg g^{-1}) (see Fig. 4b) (Liu et al. 2018). In addition, Cao et al. prepared rGO-PDA aerogel reinforced by CS and modified by 1*H*,1*H*,2*H*,2*H*-perfluorodecanethiol (PFDT) for oil–water separation (see Fig. 4c) (Cao et al. 2017).

Other methods

Coating GO sheets into the 3D porous polymers templates, such as sponge (Liu et al. 2015; Ren et al. 2017; Zhu et al. 2016a), is a convenient and efficient technology to fabricate 3DGBAs, and such materials show good oil-spill cleanup abilities because of their outstanding physical properties. For

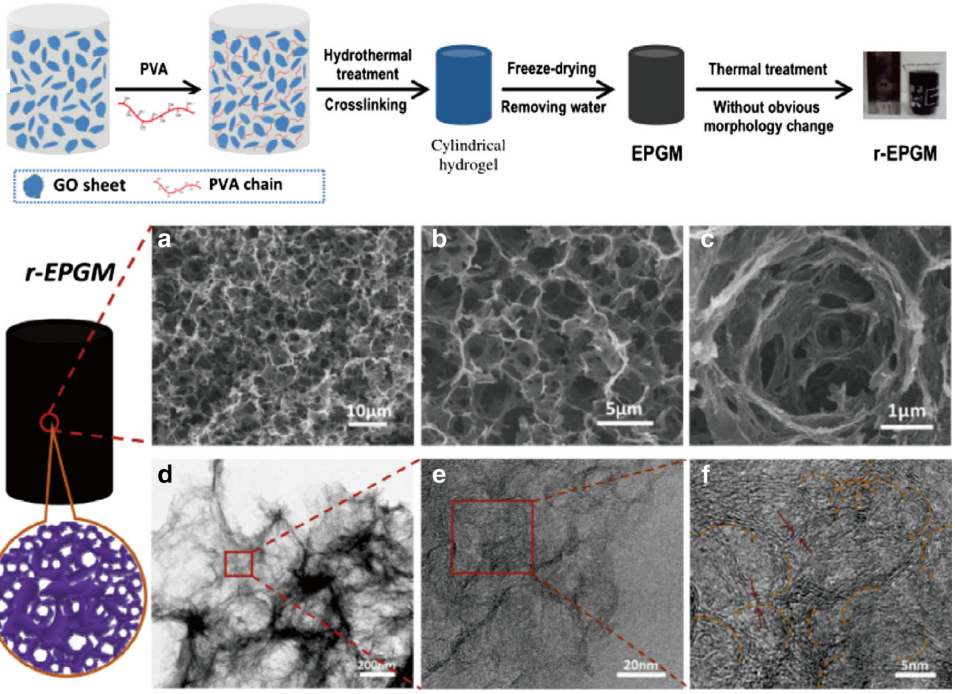

Fig. 3 Schematic showing the procedure for the preparation of r-EPGM: SEM (**a**–**c**) and TEM (**d**–**f**) images of r-EPGM (on the left is a schematic of the spheroidal and hierarchical pore structure model for r-EPGM) (Tao et al. 2014)

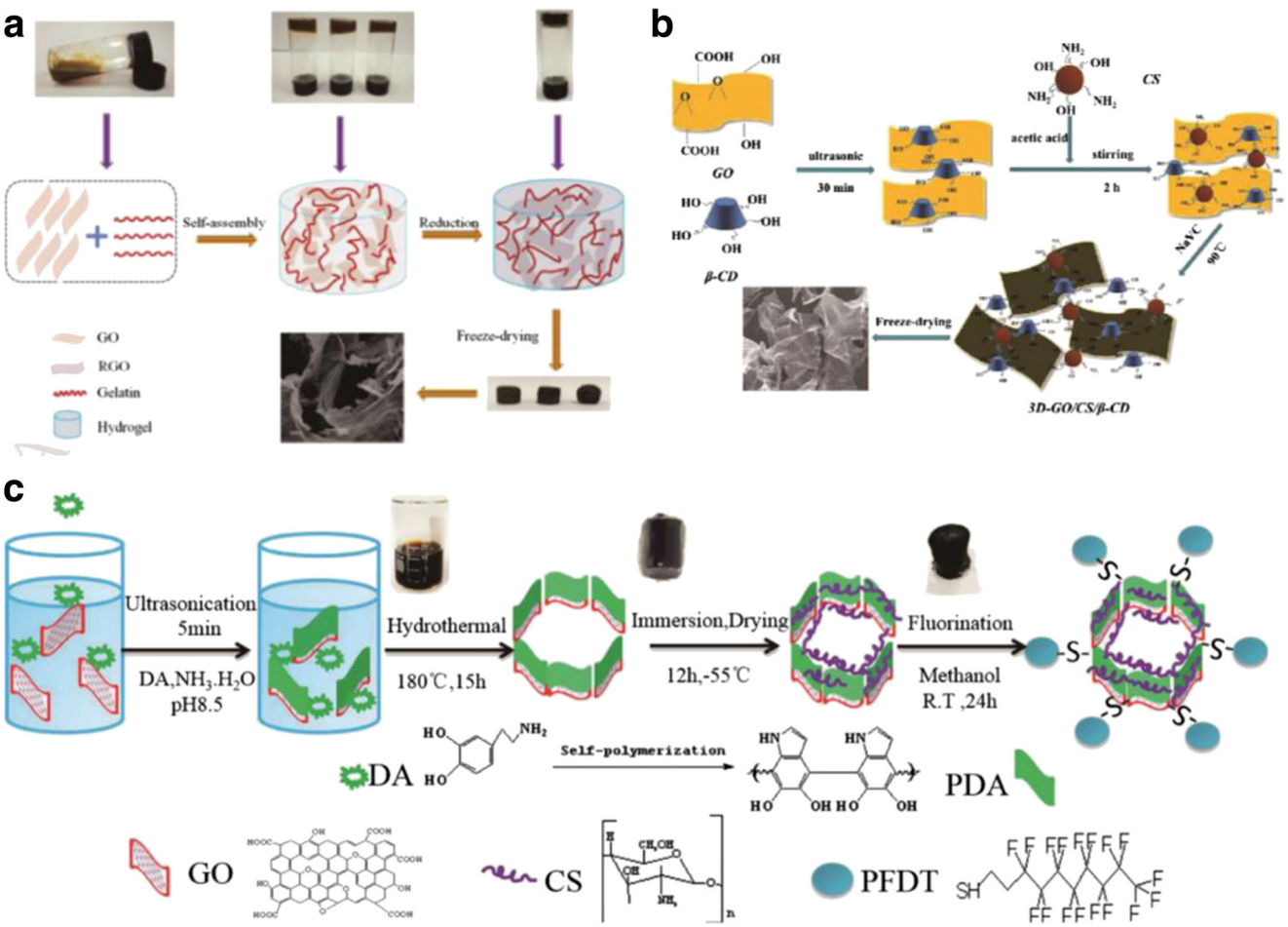

Fig. 4 **a** The proposed preparation process of GRGO (Liu et al. 2017a); **b** schematic showing the procedure for the preparation of 3D β-cyclodextrin/CS functionalized GO hydrogels (Liu et al. 2018); **c** schematic illustration of the preparation of 3D PDA/CS/rGO (Cao et al. 2017)

example, a porous polyurethane (PU)@rGO sponge for oil–water separation was fabricated by coating the rGO on the PU sponge skeletons with nanosized porous framework after etching the nano-$CaCO_3$, and the detail preparation procedure is shown in Fig. 5a (Zhu et al. 2016a). The as-prepared 3D PU@rGO sponges possessed high physical strength, hydrophobic performance, and excellent electrical conductivity because of the unique binary structure and combination the superiorities of graphene and PU foams. Moreover, the 3D sponges can be used to adsorb oil in water or break up oil-in-water emulsions via electrochemical technique. Similarly, Ali Pourjavadi's group prepared a 3D GO-hydrogel adsorbent with the aid of solid porogens to removal MB (Pourjavadi et al. 2016). As shown in Fig. 5b, the adsorbent was prepared by free radical polymerization of AMPS and AAm with MBA as the cross-linking agent in the presence of GO sheets and starch. To produce 3D porous adsorbents, $CaCO_3$ particle served as solid porogens were embedded in hydrogels and then removed them in the next step with hydrochloric acid (HCI) solution treatment.

Recently, phase separation technique has been developed to fabricate 3DGBAs with advantages of simple, low-cost, and environment friendly due to avoidance of the use of chemical treatment or the addition of stabilizers, for example, surfactants or high boiling point solvents that are hard to dislodge. Typically, Wang's group successfully prepared rGO/polycarbonate (PC) monolith by a thermally impacted nonsolvent-induced phase separation (see Fig. 5c) (Wang et al. 2018b). PC pellets and rGO PC pellets were firstly dissolved in tetrahydrofuran to obtain a homogenous mixture. Deionized water serving as nonsolvent was slowly dropped into the above suspension under strong stirring. The resultant solution was subjected to phase separation process at 4 °C for 24 h to form rGO/PC monolith. Due to unique micro-nanoscale binary structure, the resulting rGO/PC not only had the increased surface roughness but also possessed a lot of air pockets (microscopic pores) as barriers to reduce the contact area between monolith, which made rGO/PC exhibit superhydrophobicity and superoleophilicity, and have great potential for oil/water separation.

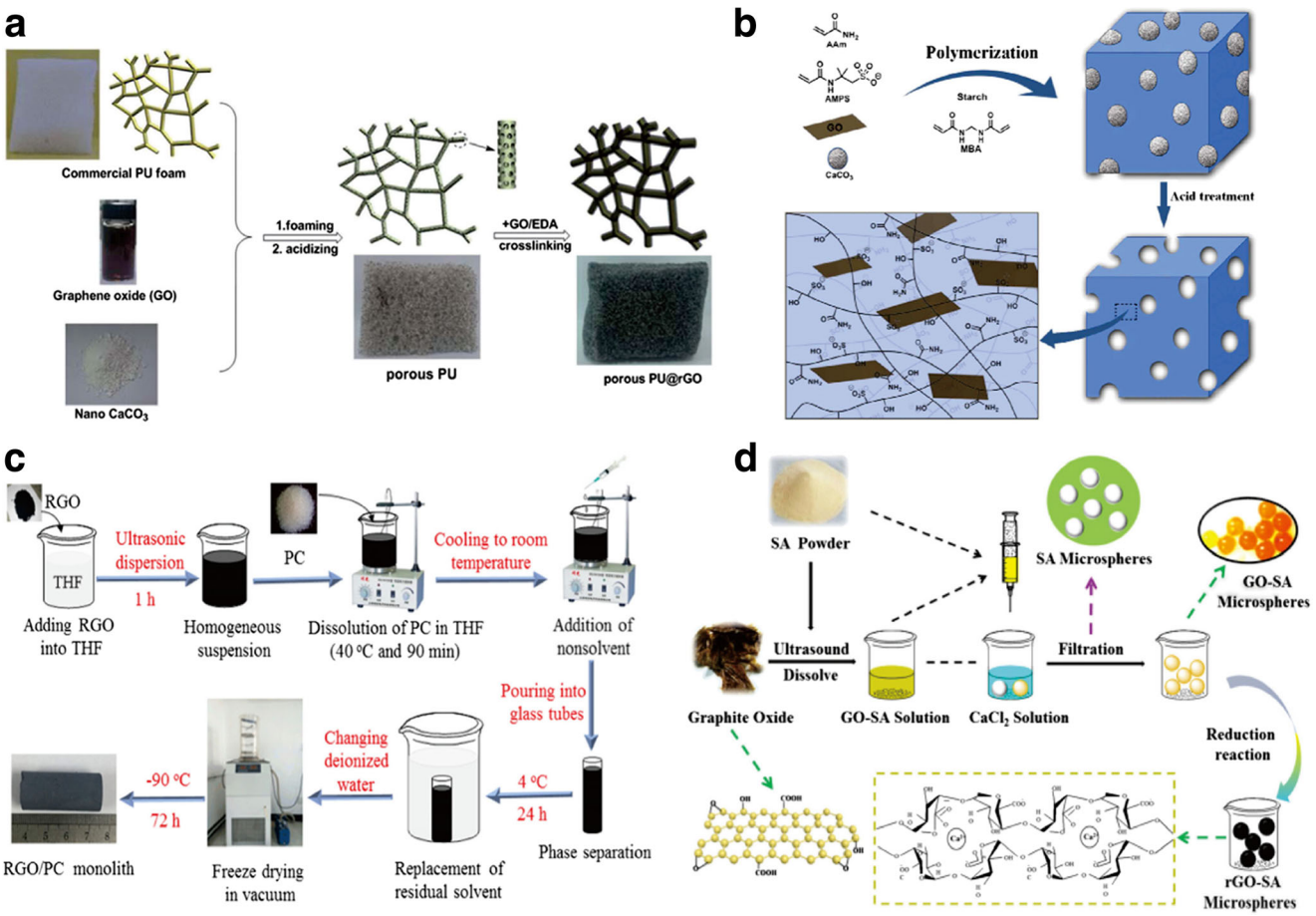

Fig. 5 **a** Schematic depiction of the fabrication of porous PU@rGO (Zhu et al. 2016a); **b** preparation of porous nanocomposite hydrogel (Pourjavadi et al. 2016); **c** fabrication procedure of porous rGO/PC monoliths (Wang et al. 2018b); **d** preparation process of rGO-SA hydrogel microspheres (Feng et al. 2017)

Moreover, an external emulsification method was reported to fabricate rGO-alginate (SA) hydrogel microspheres, and the overall preparation procedure is shown in Fig. 5d (Feng et al. 2017). Due to abundant oxygen containing groups, SA could rapidly cross-link with the bivalent cations (Ca^{2+}) to form the 3D porous network. Therefore, when the mixture solution of GO-SA was dropped into $CaCl_2$ solution, SA at the outside layer of drops turned into gels membrane rapidly, and the inside sol gradually became gel to form the SA hydrogel microspheres as the Ca^{2+} diffused into the inside of drops. The process of gel coagulation was very fast, and the particle size of microspheres can be controlled by changing the size of liquid drops.

Assembling of 3D graphene/inorganic nanomaterials adsorbents

To date, extensive researches suggest that 3DGBAs involving graphene-loaded metallic or inorganic nonmetallic nanomaterials have been successfully assembled, and these complex structures have a tremendous ascendency that is effective in the avoidance of agglomerating inorganic nanoparticles and restacking of graphene sheets, which makes uniform dispersion of nanomaterials in 3D graphene networks (Wan et al. 2016). Besides, another important advantage is that the 3D porous structures possess a great deal of surface wrinkled graphene sheets and large specific surface area, which can provide more effective attachment sites for inorganic nanomaterials in the same volume range and further offset the main disadvantage of nanoparticles in environmental protection application. The synthesis of 3D graphene/inorganic adsorbents mainly depends on the self-assembly method, and some other methods are also used, such as precipitation method (Chen et al. 2013c; Lingamdinne et al. 2017), interfacial coordination-assisted synthesis method (Yang et al. 2015b), and metal etching method (Zhang et al. 2016). In general, inorganic nanocomposites as functional components mainly cover metal particles (Ni (Zhao et al. 2015a)), metal oxides (TiO_2 (Li et al. 2016b; Wang et al. 2016, 2017b; Zhang et al. 2013c, 2018; Zhao et al. 2015b), SiO_2 (Hao et al. 2012), ZnO (Qin et al. 2015), MnO_2 (Liu et al. 2016b; Ren et al. 2011), Nd_2O_3 (Pan et al. 2018), Fe_2O_3 (Zhang et al. 2016), and Fe_3O_4 (Guo et al. 2015; Lei et al. 2014; Singh et al. 2013; Wu et al. 2016)), metal bases ($Ni(OH)_2$ (Debata et al. 2017), $Mg(OH)_2$ (Li et al. 2011), FeOOH) (Andjelkovic et al. 2015), mineral (zeolite (Liu et al. 2017b), silicalite (Cheng et al. 2017), montmorillonite (Yan et al. 2016)), CNTs (Sui et al. 2012; Wan et al. 2016; Wu et al. 2017), etc. Table 2 gives a systematic comparison of the preparation procedure for a diversity of 3D graphene/inorganic nanomaterial adsorbents.

Self-assembly method

Self-assembly method is one of the most effective and important methods to construct 3D graphene/inorganic adsorbents and has gained extensive attention due to the flexibility and controllability about structural composition and magnitude size of 3D porous networks. During the self-assembly, GO sheets not only play the role of carbon nanomaterials but also are regarded as 2D molecules that provide considerable attachment sites for inorganic particles. In this approach, the 3D interconnected porous networks are generally formed by mixing negatively charged GO sheets as the precursor with the positive charged inorganic particles to obtain a homogeneous stable dispersed solution and then further assembling GO sheets loaded with nanoparticles during the hydrothermal or reduction process. For instance, a self-assembled magnetic reduced graphene oxide/zeolitic imidazolate framework (MRGO/ZIF) was fabricated by the electrostatic attraction and the π–π stacking between MRGO and ZIF (see Fig. 6a), which showed the excellent adsorption performance toward malachite green (MG), and the adsorption capacity was about 3000 mg g^{-1} (Lin and Lee 2016).

It is noteworthy that some photocatalytic materials, such as TiO_2 and Bi_2WO_6 (Zhang et al. 2013a), have been demonstrated to be suitable for fabricating 3DGBAs to remove pollutions by synergistic effects of adsorption and photocatalysis. For a typical example of reduction self-assembly, the TiO_2-rGO hydrogel was prepared by mixing the GO and TiO_2 with sodium ascorbate and then heating at 95 °C for 1 h (see Fig. 6b) (Li et al. 2016b). Due to load of TiO_2 onto the rGO sheets surface, the aggregating and restacking of rGO sheets were inhibited. And the cross-linking network occurred through the overlapping and coalescence among the rGO sheets to build 3D TiO_2-rGH because of the π–π conjugation. The as-prepared TiO_2-rGO hydrogel exhibited a large surface area, $•O^{2-}$, and interconnected pores that provided abundant active sites and diffusion channels for adsorbate molecules, all which performed its removing ability of Cr(VI) via the combination of adsorption and photocatalysis. For another example, a poly(vinyl pyrrolidone)-assisted one-step hydrothermal self-assemble method was developed to fabricate 3D flower-like TiO_2 microsphere/graphene composite (FT/GN) using titanium(IV) isopropoxide and GO as precursors (see Fig. 6c) (Wang et al. 2016). The FT/GN hybrids showed excellent removal effect for RhB because of the synergistic effects originating from the unique micro/nano-structure of TiO_2 and the introduction of GN, in which holes and π–π stacking were beneficial to remove the contaminant molecules by absorption, and TiO_2 promoted efficient charge transport and separation.

Table 2 The preparation procedure for a diversity of 3D graphene/inorganic nanomaterial adsorbents

Strategies	Original carbon materials	Inorganic nanomaterials	Other agent	Required maximum temperature (°C)	Process difficulties	Adsorption capacity	Reference
Self-assembly methods	Graphene oxide	Zeolitic imidazolate framework	Glucose, ethanol, $Fe(SO_4)$ solution	180	Hard	MG (~ 500 mg g^{-1})	(Lin and Lee 2016)
	Graphene oxide	TiO_2	Sodium ascorbate, polyethylene glycol	95	Easy	Cr(VI) (5.6 mg g^{-1})	(Li et al. 2016b)
	Graphene oxide	Titanium (IV) isopropoxide	Glycol, poly(vinyl pyrrolidone), ethanol	150	Hard	64.35% RhB can be absorbed in 1 h	(Wang et al. 2016)
	Graphite oxide	$KMnO_4$ powder	Glycine	160	Hard	Pb^{2+} (643.62 mg g^{-1}), Cd^{2+} (250.31 mg g^{-1}), Cu^{2+} (228.46 mg g^{-1})	(Liu et al. 2016b)
	Graphene oxide	$FeCl_3$, $FeCl_2{\cdot}4H_2O$	HCl, NaOH	180	Hard	MB (100 mg g^{-1})	(Zhang et al. 2015b)
	Graphene oxide	CNTs	Vitamin C	Heated	Easy	MB (190.9 mg g^{-1}), RhB (145.9 mg g^{-1}), Pb^{2+} (104.9 mg g^{-1})	(Sui et al. 2012)
	Graphene oxide	Diatomaceous earth	Toluene, $FeSO_4{\cdot}7H_2O$, 3-aminopropyltrimethoxysilane	90	Hard	Hg^{2+} (> 500 mg g^{-1})	(Kabiri et al. 2015)
Other methods	Graphene oxide	$Fe(NO_3)_3{\cdot}9H_2O$, $Ni(NO_3)_3{\cdot}9H_2O$	Hydrazine hydrate, nitrogen atmosphere, ethanol	80	Hard	U(VI) (~ 160 mg g^{-1}), Th(IV) (~ 100 mg g^{-1})	(Lingamdinne et al. 2017)
	Graphene oxide	$Al_2(SO_4)_3$ solution	Sodium ascorbate, urea	95	Easy	Fluoride (33.4 mg g^{-1})	(Chen et al. 2013c)
	Graphene oxide	Fe_3O_4 NPs	$ClCH_2COOH$, dopamine	Room temperature	Hard	MB (298 mg g^{-1})	(Yang et al. 2015b)
	Graphene oxide	$FeCl_3{\cdot}6H_2O$	Argon atmosphere	800	Hard	MB (216.3 mg g^{-1})	(Zhang et al. 2016)

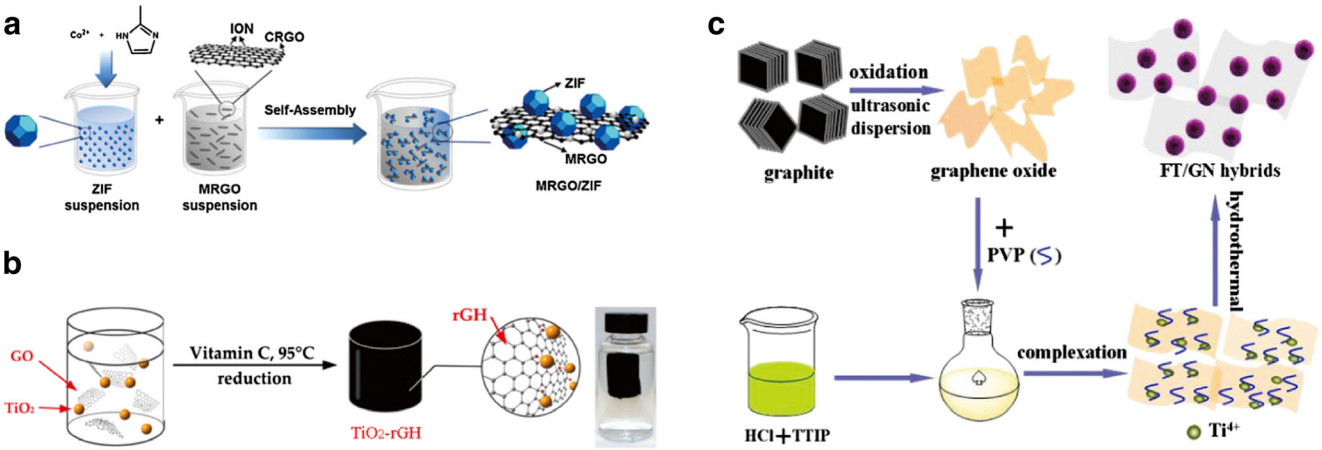

Fig. 6 **a** Synthesis scheme of MRGO/ZIF (Lin and Lee 2016). **b** Schematic illustration of the preparation process of TiO_2-rGH (Li et al. 2016b). **c** Schematic illustration for the formation of FT/GN hybrids (Wang et al. 2016)

Other methods

Using deposition phenomena of metal ions is a feasible way to prepare 3DGBAs. For example, Chang's group successfully fabricated porous rGO nickel ferrite (rGONF) nanocomposite by one pot of co-precipitation of GO sheets with nickel and iron salts (Lingamdinne et al. 2017). The detail schematic description of the preparation of rGONF is illustrated in Fig. 7a. The obtained SEM images revealed that GONF and rGONF had the porous surface morphology, which was favorable for adsorption performance. For adsorption of radionuclides (U(VI) and Th(IV)), ferromagnetic GONF and superparamagnetic rGONF were recycled for up to five cycles by magnetic separation without any significant loss of adsorption capacity. For another example, the 3D porous basic aluminum sulfate and graphene hydrogel (BAS@GHG) were fabricated by homogenous precipitation of BAS into presynthesized GHG via chemical reduction of GO (Chen et al. 2013c).

The hierarchical macro- and mesoporous 3D Fe_3O_4-GO frameworks was prepared by a novel atom-scale interfacial coordination assisted method and the scheme is shown in Fig. 7b (Yang et al. 2015b). To increase the amount of functional groups that could be used for coordination, the carboxylated GO sheets (GO-COOH) were obtained via nucleophilic substitution between the $ClCH_2COOH$ and hydroxyl groups on GO sheets in NaOH solution, and the GO-COOH reacted with dopamine (DPA) to form the phenol hydroxylated GO sheets (GO-DPA). The phenyl O atoms of GO-DPA coordinated with Fe atoms of Fe_3O_4 NPs to form the multilayer hybrid structure, and the phenyl O atoms at the edge of the multilayer hybrid further coordinated with Fe atoms of Fe_3O_4 to form the 3D Fe_3O_4-GO frameworks. Due to the incorporation of Fe_3O_4 nanoparticles, interconnected porous networks

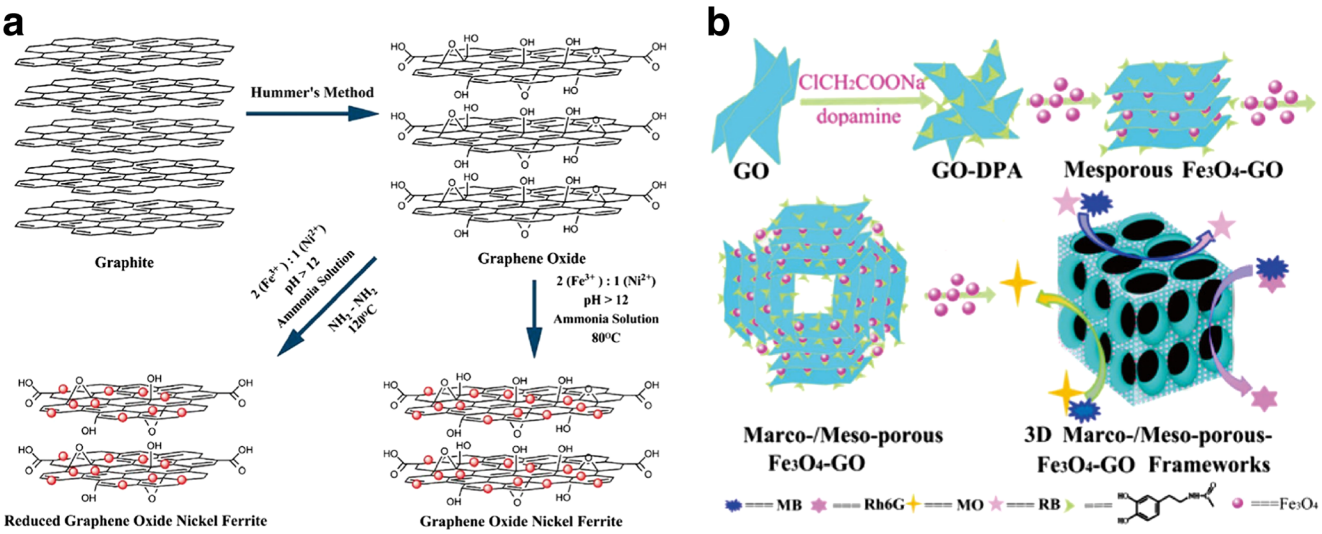

Fig. 7 **a** Schematic description of the preparation of GONF and rGONF nanocomposites (Lingamdinne et al. 2017); **b** illustration of the preparation of hierarchically porous Fe_3O_4-GO frameworks and their charge and size selective dye removal (Yang et al. 2015b)

and narrow mesopore size distribution (3–5 nm), the 3D Fe_3O_4-GO showed outstanding adsorption selective toward MB (298 mg g^{-1}) and could be easily separated from the water after adsorption. Zhang et al. designed and fabricated 3D γ-Fe_2O_3 nanocrystals anchored on unique porous graphene by metal etching approach (Zhang et al. 2016). And the samples had excellent adsorption capacity towards MB (216.3 mg g^{-1}) due to the synergistic effects of them hierarchically porous (macro- and mesopores), and interaction between graphene and MB molecules.

Environmental protection application

3D porous graphene composites have been recognized as one of the most ideal and potential materials for pollutant removal. It is known to us all that adsorption is a physicochemical process, which involves mass transfer of contaminants from liquid phase to the surface of adsorbents, and strong interaction forces between adsorbents and pollutants are indispensable for improving adsorption performance. 3DGBAs attracted substantial sight due to the following reasons. Firstly, graphene is a single layer structure, and all atoms are surface atoms, all which make 3DGBAs possess a great specific surface area and lead to easy diffusion of contaminants into the inner of adsorbents. And well-connected network and rich pores structure of 3DGBAs provide adequate transportation channels, which is also beneficial to facilitate the diffusion rate and further leads to the higher adsorption rate. Besides, a lot of work has been done to confirm that the adsorption towards pollutants onto 3DGBAs has a faster adsorption kinetics compared with the traditional adsorbents (Chen et al. 2013c; Shi et al. 2014). For example, GO-cellulose nanowhiskers nanocomposite hydrogel can efficiently remove MB and RhB, and the adsorption process revealed that 100% of MB and 90% of RhB can be removed and adsorption equilibrium was reached in 15 min (Soleimani et al. 2018). Secondly, 3D 3DGBAs can be used to remove many kinds of pollutants (for example heavy metal ions, dyes, little molecular organic pollutants, and oil) at the same time, and have relatively high adsorption capacities due to the synergetic effects of various interaction forces between 3DGBAs and contaminants (Dong et al. 2018; Gan et al. 2018; Wang and Chen 2016). For example, PDA-modified graphene hydrogel exhibited high adsorption capacities towards a wide spectrum of contaminants, such as heavy metals (Pb^{2+} and Cd^{2+}), synthetic dyes (RhB and *p*-nitrophenol), and aromatic pollutions (Gao et al. 2013). Finally, compared with other adsorption materials, 3DGBAs could be easily separated from aqueous solution due to excellent mechanical properties and showed the promising recyclability in the control of diverse contaminants (Wan et al. 2016; Yan et al. 2016).

Interaction force between 3DGNAs and contaminants mainly includes electrostatic interaction, π–π interaction, hydrophobic interaction, complexation, hydrogen bonds, and van der Waals forces. Due to electronegativity of 3DGBAs, electrostatic interaction is the main driving force for 3DGBAs to adsorb cationic pollutants, such as heavy metal ions, cationic dyes, and positive charged contaminants. Besides, the protonation of carboxyl groups will enhance in alkaline environment, which leads to the increase adsorption capacity towards cationic pollutants. The pH-dependent 3DGBAs are widely reported. For example, Lu's group revealed that the adsorption capacity of 3D Konjac glucomannan/GO hydrogel towards methyl orange (MO) and MB enhanced with the increasing pH value (Gan et al. 2015). A similar phenomenon has also been reported in many studies about 3DGBAs (Gao et al. 2013; Hosseinzadeh and Ramin 2017; Liu et al. 2016a, b, 2018; Tran et al. 2015). The π–π stacking is the interaction between the aromatic ring and the graphene structure and exists widely in the process of adsorption. Therefore, it has a great effect on the adsorbent force of 3DGBAs toward pollutants containing aromatic ring. It is worth noting that the electrostatic interaction is stronger than π–π stacking when pollutants contain the ionized groups. Typically, Yang reported that the adsorption capacity of GO toward MB was higher than adsorbents with similar structure and no negative electricity, such as rGO, peeled graphene, and CNTs, which showed that the contribution of electrostatic attraction was far greater than π–π stacking (Yang et al. 2011). The hydrophobic interaction is another important force to promote the adsorption of graphene toward pollutants, and it exists widely between the hydrophobic chain and the graphene structure. Hydrophilic pollutants, oils, and other hydrophobic pollutants can be adsorbed onto graphene through the hydrophobic interaction. If the hydrophilic pollutants contain the hydrophobic part, the hydrophobic interaction will also exist between the hydrophobic part and graphene. The complexation interaction should be considered and even carefully designed in the removal of heavy metal ions (Madadrang et al. 2012). Such the attempt has been reported in previous studies. For example, Yang decorated GO with cyanobacterium metallothionein contained sulfhydryl groups, and the resulting product showed excellent adsorption capacity towards Cd^{2+} by complexation (Yang et al. 2012). The hydrogen bonding is the interaction between the donor and the receptor of the hydrogen. The –COOH and –OH on GO sheets can provide polar oxygen connected hydrogen atoms, and these hydrogen atoms would form hydrogen bonds with other polar atoms, such as O, N, and S. But in aqueous solutions, water molecules can also provide the donor and receptor for hydrogen. So, the contribution of the hydrogen bonding to adsorption capacity is relatively small. Van der Waals forces can promote the adsorption of graphene toward pollutions, and it is effective in a large range (several hundred picometers). In aqueous solution, only

atoms with close contact will have van der Waals forces. The contribution of the van der Waals forces to adsorption capacity is small because van der Waals forces are weak for the single atom, and many pollutants contain only a small number of atoms.

According to pollutant types, the adsorption performance of 3D graphene-based composites can be roughly split into three categories, including heavy metals, dyes, oils, and organic pollutants. All of the above adsorption progress will be discussed in the following subsections in detail.

Heavy metals

Heavy metal ions (Hg^{2+} (Sui et al. 2012), Cu^{2+} (Adhikari et al. 2012; Chen et al. 2013a; Cui et al. 2018; Li et al. 2013b; Mi et al. 2012; Zhang et al. 2014b), Ag^{+} (Sui et al. 2012), Pb^{2+} (Chen et al. 2013b; Cong et al. 2012; Han et al. 2014; Li et al. 2013b), Cd^{2+} (Adhikari et al. 2012; Chen et al. 2013a; Gao et al. 2013; Li et al. 2013b; Zhang et al. 2013b, 2014b), Cr(VI) (Cong et al. 2012; Lei et al. 2014; Qin et al. 2012)) are the important pollutants in water due to their high toxicity to animals, plants, and human beings. Recent reports have demonstrated that 3DGBAs can be used to remove heavy metal ions and showed excellent adsorption properties. It is well known that 3D graphene composites are negatively charged due to the functional oxygen groups while a great majority of the heavy metals are cationic. Therefore, the content of oxygen functional groups mainly determines negative charges distributed on 3DGBAs and further affects their adsorption capacity toward heavy metals. Moreover, diverse functional components, such as CNTs (Zhang et al. 2013b), MnO_2 (Liu et al. 2016b), Mn_3O_4 (Zou et al. 2016), lignosulfonate (Li et al. 2016a), diatom silica (Kabiri et al. 2015), CS (Li et al. 2015, Zhu et al. 2016c), DNA (Cheng et al. 2013a), and BSA, have been used to insert into 3D graphene network to enhance the adsorption capacity. For instance, a 3D graphene/δ-MnO_2 exhibited outstanding adsorption capacity for Pb^{2+} (643.62 mg g^{-1}), Cd^{2+} (250.31 mg g^{-1}), and Cu^{2+} (228.46 mg g^{-1}), which was mainly because of their large surface area, interconnected pore network, and interlayer trapping effect. The adsorption capacity toward Pb^{2+} was higher than that of most adsorbents reported in the literature, such as CNTs (1.66–49.95 mg g^{-1}) (Xu et al. 2018). The 3D graphene/δ-MnO_2 aerogels also had fast adsorption kinetics and excellent regeneration toward heavy metal ions (Liu et al. 2016b). Cheng's group prepared 3D GO/biopolymers (BSA, CS, and DNA) hydrogels, and these hydrogels exhibited excellent adsorption behavior to heavy metal ions because of synergistic effects of the electrostatic attraction and the complexation between surface hydroxyl or amino groups and heavy metal ions (Cheng et al. 2013a). The adsorption amount of 3D GO/BSA, 3D GO/CS, and 3D GO/DNA to Pb^{2+} were 110, 129, and 147 mg g^{-1}, respectively, and the adsorption capacity for Cu^{2+} were 391, 370, and 480 mg g^{-1}, respectively. To further increase the adsorption selectivity of 3DGBAs, various functional components were introduced into 3DGBAs, such as SiO_2 and MoS_2 (Halouane et al. 2017; Hao et al. 2012; Zhuang et al. 2018). For example, 3D MoS_2-rGO hydrogels exhibited an excellent adsorption selectivity for Hg^{2+}, and the adsorption capacity was 340 mg g^{-1}, which was mainly because of the 3D network structure, heterointerfacial area property, and the strong soft–soft interactions between Hg and S (see Fig. 8) (Zhuang et al. 2018). Table 3 gives a systematic comparison of the adsorption properties for heavy metal ions in a diversity of 3DGBAs.

Except for the adsorption capacity, the adsorption behavior of 3DGBAs was alike in some cases. Firstly, most of the adsorption isotherms fitted the Langmuir model, which revealed that the adsorption of 3DGBAs toward heavy metals was monolayer adsorption and the active sites on 3DGBAs were uniformly distributed (Li et al. 2015; Qi et al. 2017; Shi et al. 2016c; Yang et al. 2017c). Secondly, most of the adsorption kinetics fitted the pseudo-second-order kinetic model, which suggested pseudo-second-order adsorption theory was primary when adsorption was allowed in the chemical reaction. Thirdly, the adsorption of 3DGBAs toward heavy metal ions lacked selectivity. The adsorption amount was mainly determined by some nonspecificity, such as electrostatic interaction. And the oxygen content of 3DGBAs can obviously affect the adsorption performance. Therefore, to improve the specificity and selectivity of adsorbents, 3DGBAs must be purposefully functionalized.

Dyes

A great deal of importance has been attached to the treatment and disposal of dye-containing wastewater problems. According to the presented electric charge types in water, organic dye pollutants can be categorized into two aspects including cationic dyes (MB, safranin O, MG, brilliant green (BG), MV, and RhB) and anionic dyes (methyl orange (MO), calcein (CA), rose Bengal sodium salt (RB)). Due to the electronegativity of 3DGBs, the ability of 3DGBAs to adsorb

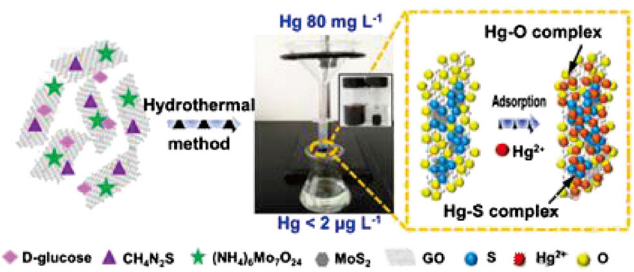

Fig. 8 A novel 3D MoS_2-rGO hydrogel with two-dimensional heterointerfaces is fabricated by an eco-friendly one-pot hydrothermal method for high selective Hg^{2+} scavenging (Zhuang et al. 2018)

Table 3 The adsorption performance of 3DGBAs for heavy metal ions

Adsorbent	Synthesis methods	Adsorption performance to heavy metal ions	Adsorption model	Reference
SiO_2/graphene composite	Cross-linking	Pb^{2+} (113.6 mg g^{-1})	Pseudo-second-order kinetic model, Langmuir isotherm model	(Hao et al. 2012)
Graphene/FeOOH aerogels	Self-assembled	Cr(VI) (139.2 mg g^{-1}), Pb^{2+} (373.8 mg g^{-1})	–	(Cong et al. 2012)
Graphene–c-MWCNT	Reduction self-assembly supercritical CO_2 drying	104.9 mg g^{-1} for Pb^{2+}, 93.3 mg g^{-1} for Hg^{2+}, 64 mg g^{-1} for Ag^{+}, and 33.8 mg g^{-1} for Cu^{2+}	–	(Sui et al. 2012)
Graphene–MWCNT hybrid aerogel	Reduction self-assembly supercritical CO_2 drying	44.5 mg g^{-1} for Pb^{2+}, 75.6 mg g^{-1} for Hg^{2+}, 46 mg g^{-1} for Ag^{+}, and 9.8 mg g^{-1} for Cu^{2+}	–	(Sui et al. 2012)
3D GO/BSA, 3D GO/CS, 3D GO/DNA	Cross-linking	Pb^{2+}, 110, 129, and 147 mg g^{-1}, respectively; Cu^{2+}, 391, 370, and 480 mg g^{-1}, respectively	–	(Cheng et al. 2013a)
Magnetic graphene oxide (MGO)	Coprecipitation	Cd^{2+} (91.29 mg g^{-1}), the time required to reach the equilibrium was 165 min for Cd^{2+}, the removal efficiencies were 33.78% for Cd^{2+}	Pseudo-second-order kinetic model, Langmuir isotherm model	(Deng et al. 2013)
Sulfonated magnetic graphene oxide composite (SMGO)	Coprecipitation	Optimum Cu^{2+} uptake of 62.73 mg g^{-1} was achieved at pH 4.68, Cu^{2+} concentrations 73.71 mg g^{-1}, and temperature 50 °C	Pseudo-second-order kinetic model, Langmuir isotherm model	(Hu et al. 2013b)
Graphene-CNT aerogels	Reduction self-assembly	Pb^{2+} (230–451 mg g^{-1})	–	(Zhang et al. 2013b)
Poly3-aminopropyltriethoxysilane (PAS)-GO	Cross-linking	Pb^{2+} (312.5 mg g^{-1}), Pb^{2+}, and Cu^{2+} were preferentially removed	Langmuir isotherm model	(Luo et al. 2014)
Graphene aerogels	Reduction self-assembly	Pb^{2+} (80 mg g^{-1}), which could reach as 5000 g m^{-3} per unit volume	–	(Han et al. 2014)
Graphene–diatom silica aerogels	Self-assembled	> 500 mg g^{-1} for Hg^{2+}, 368.0 ± 2 m^2 g^{-1}	Pseudo-second-order kinetic model, Langmuir isotherm model	(Kabiri et al. 2015)
Graphene/δ-MnO_2 aerogels	Reduction self-assembly	Pb^{2+} (643.32 mg g^{-1}), Cd^{2+} (250.31 mg g^{-1}), Cu^{2+} (228.46 mg g^{-1}), eight cycles without obvious degradation of performance	Langmuir isotherm model	(Liu et al. 2016b)
Graphene oxide-based inverse spinel nickel ferrite	Self-assembled	Pb^{2+} (25.0 mg g^{-1}) and Cr(IV) (45.50 mg g^{-1}) can be reused up to three cycles repeatedly, have a 136 m^2 g^{-1} BET surface area with a 199 m^2 g^{-1} L surface area	Pseudo-second-order kinetic model, Langmuir isotherm model	(Lingamdinne et al. 2016)
Lignosulfonate-modified graphene hydrogel	Reduction self-assembly	Pb^{2+} (1210 mg g^{-1}), removal adsorption capacities maintained ~ 90% after 5 cycles and ~ 82% after 10 cycles	Pseudo-second-order kinetic model, Langmuir isotherm model	(Li et al. 2016a)
3D MoS_2-rGO	Reduction self-assembly	Selectivity adsorption of Hg^{2+} (340 mg g^{-1}), adsorption reaches an equilibrium within 360 min	Pseudo-second-order kinetic model, Langmuir isotherm model	(Zhuang et al. 2018)

cationic dyes is generally greater than that of anions dyes. Yan et al. prepared the 3D rGO-montmorillonite aerogels and compared the adsorption performance toward anionic dyes (MO) and cationic dyes (MB) on these adsorbents (Yan et al. 2016). The adsorption capacity toward MB was higher than that of MO because the driving force of rGO of adsorbing organic dyes mainly includes π–π conjugated, electrostatic interaction, and hydrogen bond. The adsorption mechanism is shown in Fig. 9a. MB molecules were positively charged, thus the electrostatic attraction combined with the π–π conjugated drove the dye molecules into rGO-montmorillonite aerogels, resulting in their relatively higher adsorption capacity than MO. Because of the differences of the functional components, 3DGBAs showed a diverse adsorption capacities toward MB (Ai and Jiang 2012; Cheng et al. 2013b; Fan et al. 2013; Fang and Chen 2014; Liu et al. 2012; Ma et al. 2014; Sui et al. 2012; Tiwari et al. 2013; Wang et al. 2012; Wei et al. 2013; Wu et al. 2013; Zhao et al. 2012). For example, 3D GO-DNA gels displayed the adsorption capacity toward MB as high as 1100 mg g^{-1} (Cheng et al. 2013a). The 3D sodium alginate cross-linked GO hydrogel had a maximum adsorption quantity of 833.3 mg g^{-1} for MB (Ma et al. 2014). And the adsorption capacity of 3D rGO hydrogel for MB was 660 mg g^{-1} (Zhang et al. 2015a). Not limited to the MB, some other dyestuff models can also be used to evaluate the adsorption performance of 3DGBAs, such as MV (Cheng et al. 2013a, b; Wang et al. 2013), amaranth (Sui et al. 2013), RhB (Gao et al. 2013; Qin et al. 2012; Sui et al. 2013), Rh6G (Fan et al. 2013; Wang et al. 2012), MG (Fan et al. 2013; Wang et al. 2013), reactive black 5 (Cheng et al. 2012), and safranine O (Xu et al. 2010). For example, Lin reported that MRGO/ZIF exhibited an ultra-high adsorption amount toward MG (~ 3000 mg g^{-1}) (Lin and Lee 2016). The high adsorption capacity of MRGO/ZIF was essentially because of aromatic imidazole rings on ZIF, which were considered to interact with the aromatic rings of MG by the π–π stacking interaction and leading to such a high adsorption capacity. As another example, the 3D GO/anionic polyacrylamide (APAM) gelatin was used to adsorb basic fuchsin and the adsorption amount reached 1034.3 mg g^{-1} (Yang et al. 2015a). The excellent adsorption performance was mainly because of the synergistic effect of porous structure, π–π conjugated, and the function groups of the 3D GO/APAM. The cations in basic fuchsin solution can easily combine with the anions of APAM via ionic bonding, and the $–NH_2$ groups in basic fuchsin also can easily combine with the polar groups in APAM via intermolecular force and hydrogen bonding (see Fig. 9b). The 3D GO/DNA hydrogel showed maximum adsorption amount of 960 mg g^{-1} toward safranine O, which was obviously higher than other carbon adsorbents (210–785 mg g^{-1} for the ordered mesoporous carbon (Xu et al. 2010)). The 3D rGO/chitosan composites exhibited an excellent removal efficiency (97.5% at a concentration of 1.0 mg mL^{-1}) toward reactive black 5 (Cheng et al. 2012). Table 4 gives a systematic comparison of the adsorption properties for dyes in a diversity of 3DGBAs.

Similarly, the adsorption of 3DGBAs toward dyes mostly followed the Langmuir model, which revealed that the active sites were distributed evenly on the 3DGBAs and the adsorption was the monolayer adsorption. And the adsorption kinetics mostly accorded with pseudo-second-order model well, which suggests pseudo-second-order adsorption theory was primary when the adsorption of dyes was allowed in the chemical reaction.

Oils and organic pollutants

The dislodging of oils and organic pollutants from aquatic systems has gained increasing commercial and academic attention due to oil industrial waste, oil spill, and organic solvent leakage accidents. Traditionally, adsorption treatment is

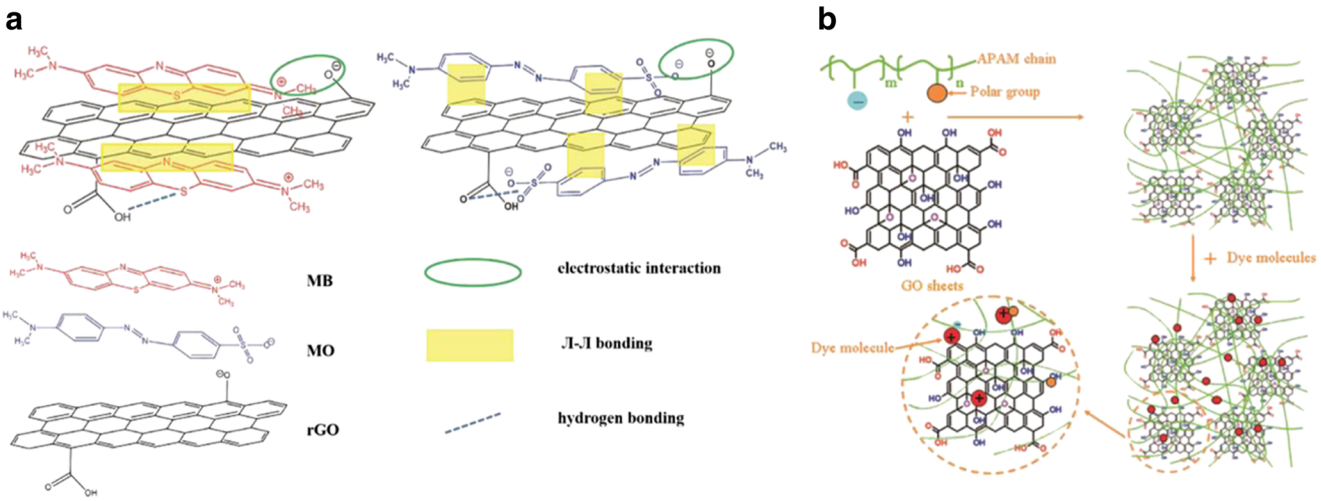

Fig. 9 **a** Mechanism of adsorption (Yan et al. 2016); **b** the schematic of the combination of APAM, GO, and basic fuchsin molecules (Yang et al. 2015a)

Table 4 The adsorption performance of 3DGBAs for dyes

Adsorbent	Synthesis methods	Adsorption performance to dyes	Adsorption model	Reference
3D GO/DNA composite hydrogels	Self-assembly	Safranine O (960 mg g^{-1})	–	(Xu et al. 2010)
3D chitosan–graphene nanocomposites	Reduction self-assembly	Specific surface area 603.2m^2 g^{-1}, removal efficiency of 97.5% at initial RB5 concentrations of 1.0 mg mL^{-1}	–	(Cheng et al. 2012)
Porous GO-biopolymer gels	Cross-linking	MB (1100 mg g^{-1}), MV (1350 mg g^{-1})	Pseudo-second-order kinetic model, Langmuir isotherm model	(Cheng et al. 2013a)
RGO-based hydrogels	Chemical reduction	MB (7.85 mg g^{-1}), RhB (29.44 mg g^{-1}), removal capabilities for MB (100%) and RhB (97%)	Pseudo-second-order kinetic model	(Tiwari et al. 2013)
3D TiO_2-graphene hydrogel	Reduction self-assembly	MB (120 mg g^{-1}), the adsorption capacity decreases down to 3% of the original value after five cycles	–	(Zhang et al. 2013c)
GO/calcium alginate composites	Cross-linking	MB (181.81 mg g^{-1})	Pseudo-second-order kinetic model, Langmuir isotherm model	(Li et al. 2013c)
3D GO–PEI porous materials	Cross-linking	Amaranth (800 mg g^{-1})	Pseudo-second-order kinetic model	(Sui et al. 2013)
3D GO–SA monolithic gel	Cross-linking	The maximum adsorption capacity from the Langmuir isotherm equation reached 833.3 mg g^{-1} for GO–SA to MB	Pseudo second-order and intra-particle diffusion models	(Ma et al. 2014)
rGO/Fe_3O_4 composites	In situ deposition of Fe_3O_4 nanoparticles	For cationic MLB, the removal rate can reach nearly 100% (after the 6th round); for cationic RhB, the removal rate can reach above 60% in the 6th round	Pseudo-second-order kinetic model	(Jiao et al. 2015)
3D rGO/L-Cys hydrogel	Reduction self-assembly	MB (660 mg g^{-1})	–	(Zhang et al. 2015a)
3D GO/APAM gel	Self-assembly	Basic fuchsin (1034.3 mg g^{-1})	Pseudo-second-order kinetic model, Langmuir isotherm model	(Yang et al. 2015a)
γ-Fe_2O_3 @P-graphene	Metal etching approach	MB (216.3 mg g^{-1}), equilibrium adsorption capacity reaches 125.1 mg g^{-1} within 0.5 min, removal efficiency is 95.3% at 1 min	Pseudo-second-order kinetic model, Langmuir isotherm model	(Zhang et al. 2016)
Magnetic reduced graphene oxide/zeolitic imidazolate framework	Self-assembly	Malachite green (~ 3000 mg g^{-1})	Pseudo-second-order kinetic model, Langmuir isotherm model	(Lin and Lee 2016)
GO/silicalite-1 composites	Grafting GO onto acid-treated silicalite-1 zeolite	The adsorption capacity for RhB was greatest at pH 3, reaching an equilibrium within 60 min, resulting in maximum adsorption capacities of 56.55 mg g^{-1}	Pseudo-second-order kinetic model, Langmuir isotherm model	(Cheng et al. 2017)
3D agar/GO aerogel	Cross-linking	MB (565.82 mg g^{-1}), retain over 91% of the adsorption capacity after recycling three times	Pseudo-second-order kinetic model, Langmuir isotherm model	(Chen et al. 2017)
3D GRGO aerogel	Reduction self-assembly	RB (280.8 mg g^{-1})	Pseudo-second-order kinetic model, Langmuir isotherm model	(Liu et al. 2017a)
RGO/Nd_2O_3 aerogels	Reduction self-assembly	RB (197.42 mg g^{-1}), ID (397 mg g^{-1}), adsorption efficiency are 88% and 92% as at the 8th recycled time for RB and ID, respectively	Pseudo-second-order model	(Pan et al. 2018)

regarded as an extremely convenient and environmentally friendly approach. In virtue of intrinsic hydrophobic nature and porosity, connected with the superiorities of functional components, 3DGBAs possess outstanding adsorptivities for various oils such as diesel, motor oil, pump oil, olive oil, gasoline, and crude oil, as well as organic pollutants such as tetrahydrofuran (THF), *N*,*N*-dimethyl formamide (DMF), chloroform, pesticides, antibiotic, phenolic compounds, and

polycyclic aromatic hydrocarbons. RGO with low oxygen content and graphene is more hydrophobic than GO, so they are easier to adsorb oils and organic pollutants. For example, graphene/α-FeOOH hydrogels with elegant microstructures were prepared by hydrothermal self-assembly method, which exhibited high capability (92% of the first maximum) for removal of oils from water after 8 cycles because of the robust interconnected network and stable porous structure (Andjelkovic et al. 2015). Strongly hydrophobic π–π stacking/coupling interactions played an important role on the adsorption process. As another example, the 3D graphene–polypyrrole composite, possessing highly delocalized π electron on the surface of graphene because of the sp^2 hybridization of carbon atoms, was covalently assembled via a hydrothermal reduction method, which led these composites to readily couple with other conjugated or nonpolar molecules (Li et al. 2013a). Typically, for aromatic compounds such as toluene and benzene, π–π stacking would result. And with hydrocarbons such as kerosene and diesel, the graphene–polypyrrole composite could adsorb these molecules by van der Waals forces. Because of these interactions and special 3D porous structure, graphene–polypyrrole composite had high sorption capacities for oil (> 100 g g^{-1}). In addition, another significant advantage of 3D graphene-based composites for oils and organic pollutants is the high adsorption rate due to their large contact surface with organic molecules and the rich pore structures. For example, Liu et al. prepared the boron codoped graphene aerogels, which had a high and rapid absorption for dodecane (see Fig. 10), and also had excellent adsorption capacities toward oil spills and organic pollutions (Liu et al. 2017c). The outstanding absorption performance could be attributed to the porous structure, large hydrophobic surface area of the rGO, and the abundant amount of adsorption active sites provided by considerably larger nitrogen, boron, and hydroxyl groups. As another example, graphene aerogels formed via reduction self-assembly method with ethylenediamine showing a high adsorption rate for *n*-dodecane (27 g/(g·s); Li et al. 2014b). The ultraflyweight aerogels were fabricated by freeze-drying mixture of CNTs and GO sheets, followed by chemical reduction of GO sheets to graphene, and its average adsorption for toluene at rates of up to 68.8 (g/(g·s); Sun et al. 2013). More importantly, due to the pore structure of the graphene sponges and its hydrophobicity, graphene sponges can float on the surface of water, which makes them very suitable for practical use. Table 5 gives a systematic comparison of the adsorption properties for oils and organic pollutants in a diversity of 3DGBAs.

Conclusions and outlook

In this review article, the recent progresses on the 3DGBAs with two hybrid systems (3D graphene/polymers and graphene/inorganic nanomaterials) have been summarized. These 3DGBAs have been extensively utilized for removal sundry contaminants, such as heavy metals, dyes, oils, and organic pollutants, via electrostatic interaction, π–π interaction, hydrophobic interaction, complexation, hydrogen bonds, and van der Waals forces. Adsorption isotherm fitted the Langmuir model and adsorption kinetics data fitted the pseudo-second-order model.

In order to promote future research and practical application, more efforts should be exerted for the following challenges. Firstly, not limited to the 3D graphene/polymer materials, the researches in the 3D graphene/inorganic nanocomposites such as 3D graphene/CNT or 3D graphene/metal oxide remain in the initial stage, and various polymers and inorganic nanoparticles should be further studied for improving the functions and application capabilities of graphene-based adsorbents. Secondly, the recyclability of 3DGBAs, involving adsorption and desorption process, is worth intensive study. The reasonable optimization could make the interaction strength between functional components and graphene sufficient to adsorb pollutants and would not lead to the difficulty of desorption, which enormously reduces the use cost of adsorbents. Thirdly, to date, adsorption properties of 3DGBAs

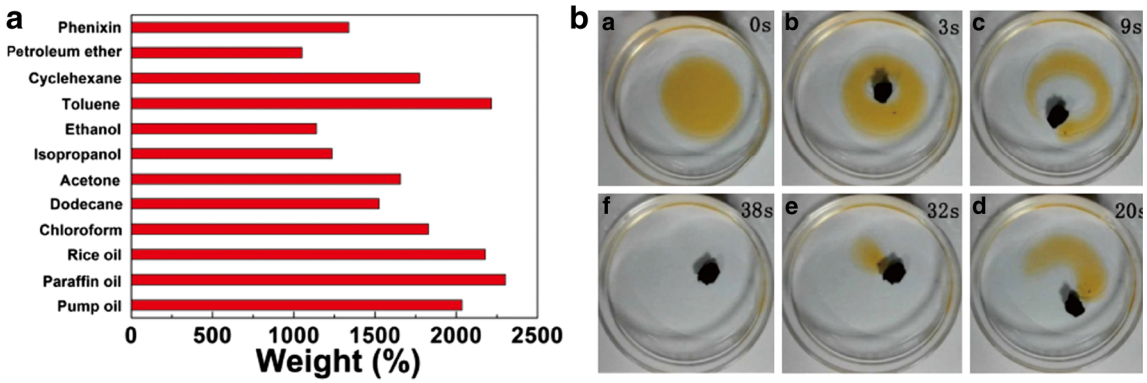

Fig. 10 **a** Adsorption capacities of the boron codoped graphene aerogels for various oils and organic solvents. **b** Absorption of dodecane from water with the boron codoped graphene aerogels (the dodecane was dyed with Sudan red for clear observation) (Liu et al. 2017c)

Table 5 The adsorption performance of 3DGBAs for oils and organic pollutants

Adsorbent	Synthesis methods	Density (mg cm^{-3})	Surface area (m^2 g^{-1})	Water contact angle (°)	Others	Adsorption capacities	Adsorption rates	Recycling	Reference
3D rGO/polypyrrole foam	Hydrothermal method	7–10	581	–	Pore diameter < 564.6 nm, total pore volume (0.46 cm^3 g^{-1})	Oil > 100 g g^{-1}, organic > 35 g g^{-1}	–	–	(Li et al. 2013a)
RGPU sponge	Coated rGO into PU sponges	0.0088	–	127	Porosity 99.29 vol.%, compressive strength decreased by 40% (400 cycles)	–	–	–	(Liu et al. 2013)
3D rGO/polyvinylidene	Solvothermal reduction	29.8–35.3	–	153.66	Young's modulus (12.6–57.3 kPa)	~ 20–70 g g^{-1} for various oils and organic solvents	Took 0.32 s to absorb a drop of dodecane	Heating (10 cycles)	(Li et al. 2014c)
3D rGO/PU foam	Self-assembly	–	–	133.4–141.1	–	Oil–water separation ~ 90%	–	–	(Hu et al. 2014)
RGO/melamine composite sponges (GM)	Template method	–	–	–	Can support a weight of 100 g with slight deformation	Diesel oil (99.0 g g^{-1})	–	Desorption in ethanol (50 cycles)	(Liu et al. 2015)
3D rGO/ poly (acrylic acid)	Cross-linking and reduction	~ 3–10	–	–	Porosity (> 99%), can support up 10,000 times their weight	All the organic liquids tested were > 100 g g^{-1} and reached a maximum of 150 g g^{-1} for pump oil	–	–	(Ha et al. 2015)
Graphene-CNTs aerogels	Hydrothermal redox reaction	6.2–12.8	–	–	–	*n*-Hexane (100–270 times its weight)	–	Burning (10 cycles)	(Wan et al. 2016)
Fluorinated PDA/CS/rGO aerogel	Self-assembly	0.08	51.76–58.19	155–165	Pore volume (0.15–0.34 cm^3 g^{-1}), pore diameter (4–40 nm)	7–20 g g^{-1} for ethanol, gasoline, acetone, diesel, hexane, toluene	Oil droplets were adsorbed within 1.4 ± 0.05 s	Extrusion and dissolved in ethanol (10 cycles)	(Cao et al. 2017)
Graphene modified foam	Coating rGO into melamine foam	–	–	–	–	High adsorption capacity (up to 140 times its own weight)	–	Good recyclability (more than 50 cycles)	(Ren et al. 2017)
RGO/CNTs	Hydrothermal assembly	4.1 ± 0.3	–	152.4 ± 2.3	–	All oily liquids were over 100.0 g g^{-1} with a maximum value of 322.8 ± 8.3 g g^{-1} of ODCB	–	> 90% adsorption capacity remained (hexadecane) after 10 runs	(Wang et al. 2017a)
Boron codoped graphene aerogels	Solvothermal method	–	–	–	–	~ 10 to 23 times to their own weight	–	–	(Liu et al. 2017c)

mainly are evaluated by models, which is feasible at the initial stage of the research. With the accumulation of basic data, such as adsorption capacity, dynamics, thermodynamics, and influencing factors, the study about 3DGBAs should be pushed toward a higher level, in which combining adsorbents with the actual pollutant samples, attentive exploring the conditions of adsorption and desorption, and monitoring the quality of water after adsorption by enrich analysis techniques are all key. Finally, the biological safety of 3DGBAs is a critical issue for their practical application and should be paid more attention. According to a related research report, graphene has low toxicity to cells, bacteria, animals, and plants, which should be avoided to release graphene to the environment during the production, transportation, use, and recycling process (Mogharabi et al. 2014). With the cross-sectoral and interdisciplinary work, we believe that 3DGBAs would reclaim development chances in multifarious field in the foreseeable future.

Acknowledgements This work was supported by the Natural Science Foundation of China (No. 51502202) and Tianjin Research Program of Application Foundation and Advanced Technology (Nos. 17JCTPJC47600 and 15JCQNJC42400).

References

Adhikari B, Biswas A, Banerjee A (2012) Graphene oxide-based hydrogels to make metal nanoparticle-containing reduced graphene oxide-based functional hybrid hydrogels. ACS Appl Mater Interfaces 4:5472–5482

Ai L, Jiang J (2012) Removal of methylene blue from aqueous solution with self-assembled cylindrical graphene-carbon nanotube hybrid. Chem Eng J 192:156–163

Andjelkovic I, Tran DNH, Kabiri S, Azari S, Markovic M, Losic D (2015) Graphene aerogels decorated with alpha-FeOOH nanoparticles for efficient adsorption of arsenic from contaminated waters. ACS Appl Mater Interfaces 7:9758–9766

Bai H, Li C, Wang X, Shi G (2010) A pH-sensitive graphene oxide composite hydrogel. Chem Commun 46:2376–2378

Bai H, Li C, Wang X, Shi G (2011) On the gelation of graphene oxide. J Phys Chem C 115:5545–5551

Bi H, Xie X, Yin K, Zhou Y, Wan S, He L, Xu F, Banhart F, Sun L, Ruoff RS (2012) Spongy graphene as a highly efficient and recyclable sorbent for oils and organic solvents. Adv Funct Mater 22:4421–4425

Bolotin KI, Sikes KJ, Jiang Z, Klima M, Fudenberg G, Hone J, Kim P, Stormer HL (2008) Ultrahigh electron mobility in suspended graphene. Solid State Commun 146:351–355

Cao N, Lyu Q, Li J, Wang Y, Yang B, Szunerits S, Boukherroub R (2017) Facile synthesis of fluorinated polydopamine/chitosan/reduced graphene oxide composite aerogel for efficient oil/water separation. Chem Eng J 326:17–28

Chen M, Zhang C, Li X, Zhang L, Ma Y, Zhang L, Xu X, Xia F, Wang W, Gao J (2013a) A one-step method for reduction and self-assembling of graphene oxide into reduced graphene oxide aerogels. J Mater Chem A 1:2869–2877

Chen Y, Chen L, Bai H, Li L (2013b) Graphene oxide-chitosan composite hydrogels as broad-spectrum adsorbents for water purification. J Mater Chem A 1:1992–2001

Chen Y, Zhang Q, Chen L, Bai H, Li L (2013c) Basic aluminum sulfate@graphene hydrogel composites: preparation and application for removal of fluoride. J Mater Chem A 1:13101–13110

Chen L, Li Y, Du Q, Wang Z, Xia Y, Yedinak E, Lou J, Ci L (2017) High performance agar/graphene oxide composite aerogel for methylene blue removal. Carbohydr Polym 155:345–353

Cheng J-S, Du J, Zhu W (2012) Facile synthesis of three-dimensional chitosan-graphene mesostructures for reactive black 5 removal. Carbohydr Polym 88:61–67

Cheng C, Deng J, Lei B, He A, Zhang X, Ma L, Li S, Zhao C (2013a) Toward 3D graphene oxide gels based adsorbents for high-efficient water treatment via the promotion of biopolymers. J Hazard Mater 263:467–478

Cheng C, Li S, Zhao J, Li X, Liu Z, Ma L, Zhang X, Sun S, Zhao C (2013b) Biomimetic assembly of polydopamine-layer on graphene: mechanisms, versatile 2D and 3D architectures and pollutant disposal. Chem Eng J 228:468–481

Cheng Z-L, Li Y-x, Liu Z (2017) Fabrication of graphene oxide/silicalite-1 composites with hierarchical porous structure and investigation on their adsorption performance for rhodamine B. J Ind Eng Chem 55:234–243

Cong H-P, Ren X-C, Wang P, Yu S-H (2012) Macroscopic multifunctional graphene-based hydrogels and aerogels by a metal ion induced self-assembly process. ACS Nano 6:2693–2703

Cui S, Wang X, Zhang X, Xia W, Tang X, Lin B, Wu Q, Zhang X, Shen X (2018) Preparation of magnetic $MnFe_2O_4$-cellulose aerogel composite and its kinetics and thermodynamics of Cu(II) adsorption. Cellulose 25:735–751

Debata S, Das TR, Madhuri R, Sharma PK (2017) Hydrothermally synthesized reduced graphene oxide/nickel hydroxide (rGO/Ni(OH)(2)) nanocomposite: a promising material in dye removal. In: Bhattacharya S, Singh S, Das A, Basu S (Editors), 61st Dae-Solid State Physics Symposium. AIP Conference Proceedings

Deng J-H, Zhang X-R, Zeng G-M, Gong J-L, Niu Q-Y, Liang J (2013) Simultaneous removal of Cd(II) and ionic dyes from aqueous solution using magnetic graphene oxide nanocomposite as an adsorbent. Chem Eng J 226:189–200

Dizaji AK, Mortaheb HR, Mokhtarani B (2016) Noncovalently functionalized graphene oxide/graphene with imidazolium-based ionic liquids for adsorptive removal of dibenzothiophene from model fuel. J Mater Sci 51:10092–10103

Dong C, Lu J, Qiu B, Shen B, Xing M, Zhang J (2018) Developing stretchable and graphene-oxide-based hydrogel for the removal of organic pollutants and metal ions. Appl Catal B Environ 222:146–156

Fan J, Shi Z, Lian M, Li H, Yin J (2013) Mechanically strong graphene oxide/sodium alginate/polyacrylamide nanocomposite hydrogel with improved dye adsorption capacity. J Mater Chem A 1:7433–7443

Fang Q, Chen B (2014) Self-assembly of graphene oxide aerogels by layered double hydroxides cross-linking and their application in water purification. J Mater Chem A 2:8941–8951

Feng J, Ding H, Yang G, Wang R, Li S, Liao J, Li Z, Chen D (2017) Preparation of black-pearl reduced graphene oxide-sodium alginate hydrogel microspheres for adsorbing organic pollutants. J Colloid Interface Sci 508:387–395

Frank IW, Tanenbaum DM, Van der Zande AM, McEuen PL (2007) Mechanical properties of suspended graphene sheets. J Vac Sci Technol B 25:2558–2561

Gan L, Shang S, Hu E, Wah C, Yuen M, S-x J (2015) Konjac glucomannan/graphene oxide hydrogel with enhanced dyes adsorption capability for methyl blue and methyl orange. Appl Surf Sci 357:866–872

Gan L, Li H, Chen L, Xu L, Liu J, Geng A, Mei C, Shang S (2018) Graphene oxide incorporated alginate hydrogel beads for the removal of various organic dyes and bisphenol a in water. Colloid Polym Sci 296:607–615

Gao H, Sun Y, Zhou J, Xu R, Duan H (2013) Mussel-inspired synthesis of polydopamine-functionalized graphene hydrogel as reusable adsorbents for water purification. ACS Appl Mater Interfaces 5:425–432

Gao Y, Zhang Y, Zhang Y, Xie L, Li X, Su F, Wei X, Xu Z, Chen C, Cai R (2016) Three-dimensional paper-like graphene framework with highly orientated laminar structure as binder-free supercapacitor electrode. J Energy Chem 25:49–54

Gokulakrishnan N, Vinu A, Mori T, Ariga K (2007) Adsorption of protein on three dimensional large pore cage type mesoporous material. Transactions of the Materials Research Society of Japan, Vol 32, No 4, 32, 995–997 pp

Guo L, Ye P, Wang J, Fu F, Wu Z (2015) Three-dimensional Fe3O4-graphene macroscopic composites for arsenic and arsenate removal. J Hazard Mater 298:28–35

Guo X, Qu L, Zhu S, Tian M, Zhang X, Sun K, Tang X (2016) Preparation of three-dimensional chitosan-graphene oxide aerogel for residue oil removal. Water Environ Res 88:768–778

Ha H, Shanmuganathan K, Ellison CJ (2015) Mechanically stable thermally cross linked poly(acrylic acid)/reduced graphene oxide aerogels. ACS Appl Mater Interfaces 7:6220–6229

Halouane F, Oz Y, Meziane D, Barras A, Juraszek J, Singh SK, Kurungot S, Shaw PK, Sanyal R, Boukherroub R, Sanyal A, Szunerits S (2017) Magnetic reduced graphene oxide loaded hydrogels: highly versatile and efficient adsorbents for dyes and selective Cr(VI) ions removal. J Colloid Interface Sci 507:360–369

Han Z, Tang Z, Shen S, Zhao B, Zheng G, Yang J (2014) Strengthening of graphene aerogels with tunable density and high adsorption capacity towards Pb2+. Sci Rep 4

Hao L, Song H, Zhang L, Wan X, Tang Y, Lv Y (2012) SiO_2/graphene composite for highly selective adsorption of Pb(II) ion. J Colloid Interface Sci 369:381–387

Hosseinzadeh H, Ramin S (2017) Fabrication of starch-graft-poly(acrylamide)/graphene oxide/hydroxyapatite nanocomposite hydrogel adsorbent for removal of malachite green dye from aqueous solution. Int J Biol Macromol

Hu H, Zhao Z, Wan W, Gogotsi Y, Qiu J (2013a) Ultralight and highly compressible graphene aerogels. Adv Mater 25:2219–2223

Hu X-J, Liu Y-G, Wang H, Chen A-W, Zeng G-M, Liu S-M, Guo Y-M, Hu X, Li T-T, Wang Y-Q, Zhou L, Liu S-H (2013b) Removal of Cu(II) ions from aqueous solution using sulfonated magnetic graphene oxide composite. Sep Purif Technol 108:189–195

Hu H, Zhao Z, Wan W, Gogotsi Y, Qiu J (2014) Polymer/graphene hybrid aerogel with high compressibility, conductivity, and "sticky" superhydrophobicity. ACS Appl Mater Interfaces 6:3242–3249

Huang Y, Li C, Lin Z (2014) EDTA-induced self-assembly of 3D graphene and its superior adsorption ability for Paraquat using a teabag. ACS Appl Mater Interfaces 6:19766–19773

Jiao T, Liu Y, Wu Y, Zhang Q, Yan X, Gao F, Bauer AJP, Liu J, Zeng T, Li B (2015) Facile and scalable preparation of graphene oxide-based magnetic hybrids for fast and highly efficient removal of organic dyes. Sci Rep 5

Kabiri S, Tran DNH, Altalhi T, Losic D (2014) Outstanding adsorption performance of graphene-carbon nanotube aerogels for continuous oil removal. Carbon 80:523–533

Kabiri S, Tran DNH, Azari S, Losic D (2015) Graphene-diatom silica aerogels for efficient removal of mercury ions from water. ACS Appl Mater Interfaces 7:11815–11823

Kemp KC, Seema H, Saleh M, Le NH, Mahesh K, Chandra V, Kim KS (2013) Environmental applications using graphene composites: water remediation and gas adsorption. Nanoscale 5:3149–3171

Kondo A, Daimaru T, Noguchi H, Ohba T, Kaneko K, Kanob H (2007) Adsorption of water on three-dimensional pillared-layer metal organic frameworks. J Colloid Interface Sci 314:422–426

Lei Y, Chen F, Luo Y, Zhang L (2014) Three-dimensional magnetic graphene oxide foam/Fe3O4 nanocomposite as an efficient absorbent for Cr(VI) removal. J Mater Sci 49:4236–4245

Li D, Mueller MB, Gilje S, Kaner RB, Wallace GG (2008) Processable aqueous dispersions of graphene nanosheets. Nat Nanotechnol 3: 101–105

Li B, Cao H, Yin G (2011) Mg(OH)(2)@reduced graphene oxide composite for removal of dyes from water. J Mater Chem 21: 13765–13768

Li H, Liu L, Yang F (2013a) Covalent assembly of 3D graphene/polypyrrole foams for oil spill cleanup. J Mater Chem A 1: 3446–3453

Li W, Gao S, Wu L, Qiu S, Guo Y, Geng X, Chen M, Liao S, Zhu C, Gong Y, Long M, Xu J, Wei X, Sun M, Liu L (2013b) High-density three-dimension graphene macroscopic objects for high-capacity removal of heavy metal ions. Sci Rep 3

Li Y, Du Q, Liu T, Sun J, Wang Y, Wu S, Wang Z, Xia Y, Xia L (2013c) Methylene blue adsorption on graphene oxide/calcium alginate composites. Carbohydr Polym 95:501–507

Li C, She M, She X, Dai J, Kong L (2014a) Functionalization of polyvinyl alcohol hydrogels with graphene oxide for potential dye removal. J Appl Polym Sci 131

Li J, Li J, Meng H, Xie S, Zhang B, Li L, Ma H, Zhang J, Yu M (2014b) Ultra-light, compressible and fire-resistant graphene aerogel as a highly efficient and recyclable absorbent for organic liquids. J Mater Chem A 2:2934–2941

Li R, Chen C, Li J, Xu L, Xiao G, Yan D (2014c) A facile approach to superhydrophobic and superoleophilic graphene/polymer aerogels. J Mater Chem A 2:3057–3064

Li L, Wang Z, Ma P, Bai H, Dong W, Chen M (2015) Preparation of polyvinyl alcohol/chitosan hydrogel compounded with graphene oxide to enhance the adsorption properties for Cu(II) in aqueous solution. J Polym Res 22

Li F, Wang X, Yuan T, Sun R (2016a) A lignosulfonate-modified graphene hydrogel with ultrahigh adsorption capacity for Pb(II) removal. J Mater Chem A 4:11888–11896

Li Y, Cui W, Liu L, Zong R, Yao W, Liang Y, Zhu Y (2016b) Removal of Cr(VI) by 3D TiO_2-graphene hydrogel via adsorption enriched with photocatalytic reduction. Appl Catal B Environ 199:412–423

Lin K-YA, Lee W-D (2016) Highly efficient removal of malachite green from water by a magnetic reduced graphene oxide/zeolitic imidazolate framework self assembled nanocomposite. Appl Surf Sci 361:114–121

Lingamdinne LP, Koduru JR, Choi Y-L, Chang Y-Y, Yang J-K (2016) Studies on removal of Pb(II) and Cr(III) using graphene oxide based inverse spinel nickel ferrite nano-composite as sorbent. Hydrometallurgy 165:64–72

Lingamdinne LP, Choi Y-L, Kim I-S, Yang J-K, Koduru JR, Chang Y-Y (2017) Preparation and characterization of porous reduced graphene oxide based inverse spinel nickel ferrite nanocomposite for adsorption removal of radionuclides. J Hazard Mater 326:145–156

Liu F, Chung S, Oh G, Seo TS (2012) Three-dimensional graphene oxide nanostructure for fast and efficient water-soluble dye removal. ACS Appl Mater Interfaces 4:922–927

Liu Y, Ma J, Wu T, Wang X, Huang G, Liu Y, Qiu H, Li Y, Wang W, Gao J (2013) Cost-effective reduced graphene oxide-coated polyurethane sponge as a highly efficient and reusable oil-absorbent. ACS Appl Mater Interfaces 5:10018–10026

Liu T, Zhao G, Zhang W, Chi H, Hou C, Sun Y (2015) The preparation of superhydrophobic graphene/melamine composite sponge applied in treatment of oil pollution. J Porous Mater 22:1573–1580

Liu J, Chu H, Wei H, Zhu H, Wang G, Zhu J, He J (2016a) Facile fabrication of carboxymethyl cellulose sodium/graphene oxide hydrogel microparticles for water purification. RSC Adv 6: 50061–50069

Liu J, Ge X, Ye X, Wang G, Zhang H, Zhou H, Zhang Y, Zhao H (2016b) 3D graphene/delta-MnO_2 aerogels for highly efficient and reversible removal of heavy metal ions. J Mater Chem A 4:1970–1979

Liu C, Liu H, Xu A, Tang K, Huang Y, Lu C (2017a) In situ reduced and assembled three-dimensional graphene aerogel for efficient dye removal. J Alloys Compd 714:522–529

Liu H, Yu A, Liu H, Chu S, Tan S (2017b) Preparation of graphene/zeolite composites and the adsorption of pollutants in water. Russ J Appl Chem 90:1171–1180

Liu Y, Xiang M, Hong L (2017c) Three-dimensional nitrogen and boron codoped graphene for carbon dioxide and oils adsorption. RSC Adv 7:6467–6473

Liu Y, Huang S, Zhao X, Zhang Y (2018) Fabrication of three-dimensional porous beta-cyclodextrin/chitosan functionalized graphene oxide hydrogel for methylene blue removal from aqueous solution. Colloids Surf A Physicochem Eng Asp 539:1–10

Luo S, Xu X, Zhou G, Liu C, Tang Y, Liu Y (2014) Amino siloxane oligomer-linked graphene oxide as an efficient adsorbent for removal of Pb(II) from wastewater. J Hazard Mater 274:145–155

Ma X (2016) 3D porous graphene/polyvinyl alcohol composites: the effect of modification on the adsorption properties. Nano 11:64–72

Ma Y, Chen Y (2015) Three-dimensional graphene networks: synthesis, properties and applications. Natl Sci Rev 2:40–53

Ma T, Chang PR, Zheng P, Zhao F, Ma X (2014) Fabrication of ultra-light graphene-based gels and their adsorption of methylene blue. Chem Eng J 240:595–600

Madadrang CJ, Kim HY, Gao G, Wang N, Zhu J, Feng H, Gorring M, Kasner ML, Hou S (2012) Adsorption behavior of EDTA-graphene oxide for Pb (II) removal. ACS Appl Mater Interfaces 4:1186–1193

Mi X, Huang G, Xie W, Wang W, Liu Y, Gao J (2012) Preparation of graphene oxide aerogel and its adsorption for Cu2+ ions. Carbon 50: 4856–4864

Mogharabi M, Abdollahi M, Faramarzi MA (2014) Safety concerns to application of graphene compounds in pharmacy and medicine. Daru 22(1):23

Ni Y, Chen L, Teng K, Shi J, Qian X, Xu Z, Tian X, Hu C, Ma M (2015) Superior mechanical properties of epoxy composites reinforced by 3D interconnected graphene skeleton. ACS Appl Mater Interfaces 7: 11583–11591

Pan L, Liu S, Oderinde O, Li K, Yao F, Fu G (2018) Facile fabrication of graphene-based aerogel with rare earth metal oxide for water purification. Appl Surf Sci 427:779–786

Papandrea B, Xu X, Xu Y, Chen C-Y, Lin Z, Wang G, Luo Y, Liu M, Huang Y, Mai L, Duan X (2016) Three-dimensional graphene framework with ultra-high sulfur content for a robust lithium-sulfur battery. Nano Res 9:240–248

Pourjavadi A, Nazari M, Kabiri B, Hosseini SH, Bennett C (2016) Preparation of porous graphene oxide/hydrogel nanocomposites and their ability for efficient adsorption of methylene blue. RSC Adv 6:10430–10437

Qi H, Liu H, Gao Y (2015) Removal of Sr(II) from aqueous solutions using polyacrylamide modified graphene oxide composites. J Mol Liq 208:394–401

Qi Y, Yang M, Xu W, He S, Men Y (2017) Natural polysaccharides-modified graphene oxide for adsorption of organic dyes from aqueous solutions. J Colloid Interface Sci 486:84–96

Qin S-Y, Liu X-J, Zhuo R-X, Zhang X-Z (2012) Microstructure-controllable graphene oxide hydrogel film based on a pH-responsive graphene oxide hydrogel. Macromol Chem Phys 213: 2044–2051

Qin J, Li R, Lu C, Jiang Y, Tang H, Yang X (2015) Ag/ZnO/graphene oxide heterostructure for the removal of rhodamine B by the synergistic adsorption-degradation effects. Ceram Int 41:4231–4237

Ren L, Liu T, Guo J, Guo S, Wang X, Wang W (2010) A smart pH responsive graphene/polyacrylamide complex via noncovalent interaction. Nanotechnology 21:335701

Ren Y, Yan N, Wen Q, Fan Z, Wei T, Zhang M, Ma J (2011) Graphene/delta-MnO_2 composite as adsorbent for the removal of nickel ions from wastewater. Chem Eng J 175:1–7

Ren R-P, Li W, Lv Y-K (2017) A robust, superhydrophobic graphene aerogel as a recyclable sorbent for oils and organic solvents at various temperatures. J Colloid Interface Sci 500:63–68

Rethinasabapathy M, Kang S-M, Jang S-C, Huh YS (2017) Three-dimensional porous graphene materials for environmental applications. Carbon Lett 22:1–13

Riaz MA, McKay G, Saleem J (2017) 3D graphene-based nanostructured materials as sorbents for cleaning oil spills and for the removal of dyes and miscellaneous pollutants present in water. Environ Sci Pollut Res 24:27731–27745

Shen Y, Fang Q, Chen B (2015) Environmental applications of three-dimensional graphene-based macrostructures: adsorption, transformation, and detection. Environ Sci Technol 49:67–84

Shi Y, Zhong S, Wu M, Chen J (2014) Comparing different kinds of materials for adsorption of methylene blue. In: Liu HW, Wang G, Zhang GW (Editors), Material Science, Civil Engineering and Architecture Science, Mechanical Engineering and Manufacturing Technology Ii. Applied Mechanics and Materials, pp. 1331−+

Shi J, Wu T, Teng K, Wang W, Shan M, Xu Z, Lv H, Deng H (2016a) Simultaneous electrospinning and spraying toward branch-like nanofibrous membranes functionalised with carboxylated MWCNTs for dye removal. Mater Lett 166:26–29

Shi L, Chen K, Du R, Bachmatiuk A, Ruemmeli MH, Xie K, Huang Y, Zhang Y, Liu Z (2016b) Scalable seashell-based chemical vapor deposition growth of three-dimensional graphene foams for oil–water separation. J Am Chem Soc 138:6360–6363

Shi YC, Wang AJ, Wu XL, Chen JR, Feng JJ (2016c) Green-assembly of three-dimensional porous graphene hydrogels for efficient removal of organic dyes. J Colloid Interface Sci 484:254–262

Singh K, Ohlan A, Viet Hung P, Balasubramaniyan R, Varshney S, Jang J, Hur SH, Choi WM, Kumar M, Dhawan SK, Kong B-S, Chung JS (2013) Nanostructured graphene/Fe_3O_4 incorporated polyaniline as a high performance shield against electromagnetic pollution. Nanoscale 5:2411–2420

Soleimani K, Tehrani AD, Adeli M (2018) Bioconjugated graphene oxide hydrogel as an effective adsorbent for cationic dyes removal. Ecotoxicol Environ Saf 147:34–42

Sui Z, Meng Q, Zhang X, Ma R, Cao B (2012) Green synthesis of carbon nanotube-graphene hybrid aerogels and their use as versatile agents for water purification. J Mater Chem 22:8767–8771

Sui Z-Y, Cui Y, Zhu J-H, Han B-H (2013) Preparation of three-dimensional graphene oxide–polyethylenimine porous materials as dye and gas adsorbents. ACS Appl Mater Interfaces 5:9172–9179

Sun H, Xu Z, Gao C (2013) Multifunctional, ultra-flyweight, synergistically assembled carbon aerogels. Adv Mater 25:2554–2560

Tan L, Wang Y, Liu Q, Wang J, Jing X, Liu L, Liu J, Song D (2015) Enhanced adsorption of uranium (VI) using a three-dimensional layered double hydroxide/graphene hybrid material. Chem Eng J 259:752–760

Tao Y, Kong D, Zhang C, Lv W, Wang M, Li B, Huang Z-H, Kang F, Yang Q-H (2014) Monolithic carbons with spheroidal and hierarchical pores produced by the linkage of functionalized graphene sheets. Carbon 69:169–177

Tiwari JN, Mahesh K, Le NH, Kemp KC, Timilsina R, Tiwari RN, Kim KS (2013) Reduced graphene oxide-based hydrogels for the efficient capture of dye pollutants from aqueous solutions. Carbon 56: 173–182

Tran DNH, Kabiri S, Sim TR, Losic D (2015) Selective adsorption of oil–water mixtures using polydimethylsiloxane (PDMS)-graphene sponges. Environ Sci Water Res Technol 1:298–305

Wan W, Zhang R, Li W, Liu H, Lin Y, Li L, Zhou Y (2016) Graphene-carbon nanotube aerogel as an ultra-light, compressible and recyclable highly efficient absorbent for oil and dyes. Environ Sci Nano 3:107–113

Wang P, Chen J (2016) Comparing different kinds of materials for adsorption of pollutants in wastewater. Adv Energy Environ Mater Sci: 223–225

Wang J, Shi Z, Fan J, Ge Y, Yin J, Hu G (2012) Self-assembly of graphene into three-dimensional structures promoted by natural phenolic acids. J Mater Chem 22:22459–22466

Wang Y, Zhang P, Liu CF, Huang CZ (2013) A facile and green method to fabricate graphene-based multifunctional hydrogels for miniature-scale water purification. RSC Adv 3:9240–9246

Wang N, Chang PR, Zheng P, Ma X (2014a) Graphene-poly(vinyl alcohol) composites: fabrication, adsorption and electrochemical properties. Appl Surf Sci 314:815–821

Wang X, Liu Z, Zhong H, Guo Z, Yuan X (2014b) Mussel-inspired synthesis of polydopamine-functionalized graphene oxide hydrogel as broad-spectrum antimicrobial material. In: Luo Q, Wang LV, Tuchin VV (Editors), Twelfth International Conference on Photonics and Imaging in Biology and Medicine. Proceedings of SPIE

Wang Y, Mo Z, Zhang P, Zhang C, Han L, Guo R, Gou H, Wei X, Hu R (2016) Synthesis of flower-like TiO_2 microsphere/graphene composite for removal of organic dye from water. Mater Des 99:378–388

Wang C, Yang S, Ma Q, Jia X, Ma P-C (2017a) Preparation of carbon nanotubes/graphene hybrid aerogel and its application for the adsorption of organic compounds. Carbon 118:765–771

Wang M, Cai L, Jin Q, Zhang H, Fang S, Qu X, Zhang Z, Zhang Q (2017b) One-pot composite synthesis of three-dimensional graphene oxide/poly (vinyl alcohol)/TiO_2 microspheres for organic dye removal. Sep Purif Technol 172:217–226

Wang X, Liu Q, Liu J, Chen R, Zhang H, Li R, Li Z, Wang J (2017c) 3D self-assembly polyethyleneimine modified graphene oxide hydrogel for the extraction of uranium from aqueous solution. Appl Surf Sci 426:1063–1074

Wang H, Li N, Xu Z, Tian X, Mai W, Li J, Chen C, Chen L, Fu H, Zhang X (2018a) Enhanced sheet-sheet welding and interfacial wettability of 3D graphene networks as radiation protection in gamma-irradiated epoxy composites. Compos Sci Technol 157:57–66

Wang Y, Wang B, Wang J, Ren Y, Xuan C, Liu C, Shen C (2018b) Superhydrophobic and superoleophilic porous reduced graphene oxide/polycarbonate monoliths for high-efficiency oil/water separation. J Hazard Mater 344:849–856

Wei G, Miao Y-E, Zhang C, Yang Z, Liu Z, Tjiu WW, Liu T (2013) N-doped graphene/carbon cryogels and their applications as versatile sorbents for water purification. ACS Appl Mater Interfaces 5: 7584–7591

Wu T, Chen M, Zhang L, Xu X, Liu Y, Yan J, Wang W, Gao J (2013) Three-dimensional graphene-based aerogels prepared by a self-assembly process and its excellent catalytic and absorbing performance. J Mater Chem A 1:7612–7621

Wu X-L, Shi Y, Zhong S, Lin H, Chen J-R (2016) Facile synthesis of Fe_3O_4-graphene@mesoporous SiO_2 nanocomposites for efficient removal of methylene blue. Appl Surf Sci 378:80–86

Wu L, Qin Z, Zhang L, Meng T, Yu F, Ma J (2017) CNT-enhanced amino-functionalized graphene aerogel adsorbent for highly efficient removal of formaldehyde. New J Chem 41:2527–2533

Wu H, Zhou Z, Chen L, Li W, Han Q, Li C, Xu Z, Qian X (2018) PECVD-induced growing of diverse nanomaterials on carbon nanofibers under various conditions. Mater Lett 216:291–294

Xiao J, Lv W, Xie Z, Song Y, Zheng Q (2017) L-cysteine-reduced graphene oxide/poly(vinyl alcohol) ultralight aerogel as a broad-spectrum adsorbent for anionic and cationic dyes. J Mater Sci 52: 5807–5821

Xu Y, Wu Q, Sun Y, Bai H, Shi G (2010) Three-dimensional self-assembly of graphene oxide and DNA into multifunctional hydrogels. ACS Nano 4:7358–7362

Xu Z, Zhang Y, Qian X, Shi J, Chen L, Li B, Niu J, Liu L (2014) One step synthesis of polyacrylamide functionalized graphene and its application in Pb(II) removal. Appl Surf Sci 316:308–314

Xu Y, Shi G, Duan X (2015) Self-assembled three-dimensional graphene macrostructures: synthesis and applications in supercapacitors. Acc Chem Res 48:1666–1675

Xu J, Cao Z, Zhang Y, Yuan Z, Lou Z, Xu X, Wang X (2018) A review of functionalized carbon nanotubes and graphene for heavy metal adsorption from water: preparation, application, and mechanism. Chemosphere 195:351–364

Yan X, Hu W, Guo J, Cai X, Huang L, Xiong Y, Tan S (2016) Easily separated a novel rGO-MMT three-dimensional aerogel with good adsorption and recyclable property. Chemistryselect 1:5828–5837

Yang S-T, Chen S, Chang Y, Cao A, Liu Y, Wang H (2011) Removal of methylene blue from aqueous solution by graphene oxide. J Colloid Interface Sci 359:24–29

Yang T, Liu L-h, J-w L, Chen M-L, Wang J-H (2012) Cyanobacterium metallothionein decorated graphene oxide nanosheets for highly selective adsorption of ultra-trace cadmium. J Mater Chem 22:21909–21916

Yang X, Li Y, Du Q, Sun J, Chen L, Hu S, Wang Z, Xia Y, Xia L (2015a) Highly effective removal of basic fuchsin from aqueous solutions by anionic polyacrylamide/graphene oxide aerogels. J Colloid Interface Sci 453:107–114

Yang Y, Hu G, Chen F, Liu J, Liu W, Zhang H, Wang B (2015b) An atom-scale interfacial coordination strategy to prepare hierarchically porous Fe_3O_4-graphene frameworks and their application in charge and size selective dye removal. Chem Commun 51:14405–14408

Yang X, Li Y, Du Q, Wang X, Hu S, Chen L, Wang Z, Xia Y, Xia L (2016) Adsorption of methylene blue from aqueous solutions by polyvinyl alcohol/graphene oxide composites. J Nanosci Nanotechnol 16:1775–1782

Yang L, Jia F, Yang B, Song S (2017a) Efficient adsorption of Au(CN)(2−) from gold cyanidation with graphene oxide-polyethylenimine hydrogel as adsorbent. Results in Physics 7:4089–4095

Yang M, Liu X, Qi Y, Sun W, Men Y (2017b) Preparation of kappa-carrageenan/graphene oxide gel beads and their efficient adsorption for methylene blue. J Colloid Interface Sci 506:669–677

Yang M, Liu X, Qi Y, Sun W, Yi M (2017c) Preparation of κ-carrageenan/graphene oxide gel beads and their efficient adsorption for methylene blue. J Colloid Interface Sci 506:669–677

Yang Y, Song S, Zhao Z (2017d) Graphene oxide (GO)/polyacrylamide (PAM) composite hydrogels as efficient cationic dye adsorbents. Colloids Surf A Physicochem Eng Asp 513:315–324

Yavari F, Chen Z, Thomas AV, Ren W, Cheng H-M, Koratkar N (2011) High sensitivity gas detection using a macroscopic three-dimensional graphene foam network. Sci Rep 1

Ye S, Feng J, Wu P (2013) Highly elastic graphene oxide-epoxy composite aerogels via simple freeze-drying and subsequent routine curing. J Mater Chem A 1:3495–3502

Zeng M, Wang W-L, Bai X-D (2013) Preparing three-dimensional graphene architectures: review of recent developments. Chin Phys B 22:098105

Zhang J, Huang Z-H, Xu Y, Kang F (2013a) Hydrothermal synthesis of graphene/Bi2WO6 composite with high adsorptivity and photoactivity for azo dyes. J Am Ceram Soc 96:1562–1569

Zhang M, Gao B, Cao X, Yang L (2013b) Synthesis of a multifunctional graphene-carbon nanotube aerogel and its strong adsorption of lead from aqueous solution. RSC Adv 3:21099–21105

Zhang Z, Xiao F, Guo Y, Wang S, Liu Y (2013c) One-pot self-assembled three-dimensional TiO2-graphene hydrogel with improved adsorption capacities and photocatalytic and electrochemical activities. ACS Appl Mater Interfaces 5:2227–2233

Zhang R, Cao Y, Li P, Zang X, Sun P, Wang K, Zhong M, Wei J, Wu D, Kang F, Zhu H (2014a) Three-dimensional porous graphene sponges assembled with the combination of surfactant and freeze-drying. Nano Res 7:1477–1487

Zhang Y, Liu Y, Wang X, Sun Z, Ma J, Wu T, Xing F, Gao J (2014b) Porous graphene oxide/carboxymethyl cellulose monoliths, with high metal ion adsorption. Carbohydr Polym 101:392–400

Zhang X, Liu D, Yang L, Zhou L, You T (2015a) Self-assembled three-dimensional graphene-based materials for dye adsorption and catalysis. J Mater Chem A 3:10031–10037

Zhang Z, Dong Y, Xiao F, Wang S (2015b) Multifunctional magnetic graphene hybrid architectures: one-pot synthesis and their applications as organic pollutants adsorbents and supercapacitor electrodes. RSC Adv 5:83480–83485

Zhang LY, Zhang W, Zhou Z, Li CM (2016) Gamma-Fe2O3 nanocrystals-anchored macro/meso-porous graphene as a highly efficient adsorbent toward removal of methylene blue. J Colloid Interface Sci 476:200–205

Zhang Y, Cui W, An W, Liu L, Liang Y, Zhu Y (2018) Combination of photoelectrocatalysis and adsorption for removal of bisphenol a over TiO2-graphene hydrogel with 3D network structure. Appl Catal B Environ 221:36–46

Zhao J, Ren W, Cheng H-M (2012) Graphene sponge for efficient and repeatable adsorption and desorption of water contaminations. J Mater Chem 22:20197–20202

Zhao J, Wang Z, White JC, Xing B (2014) Graphene in the aquatic environment: adsorption, dispersion, toxicity and transformation. Environ Sci Technol 48:9995–10009

Zhao C, Guo J, Yang Q, Tong L, Zhang J, Zhang J, Gong C, Zhou J, Zhang Z (2015a) Preparation of magnetic Ni@graphene nanocomposites and efficient removal organic dye under assistance of ultrasound. Appl Surf Sci 357:22–30

Zhao H, Yu H, Qiu F, Li X (2015b) Chitosan/graphene/TiO2 composites: preparation and its application for removal of Cr(VI). In: Choi SB (Editor), Proceedings of the 2015 International Forum on Energy, Environment Science and Materials. AER-Advances in Engineering Research, pp. 914–917

Zhou G, Ye Z, Shi W, Liu J, Xi F (2014) Applications of three dimensional graphene and its composite materials. Prog Chem 26: 950–960

Zhu C, Han TY-J, Duoss EB, Golobic AM, Kuntz JD, Spadaccini CM, Worsley MA (2015) Highly compressible 3D periodic graphene aerogel microlattices. Nat Commun 6:6962

Zhu H, Chen D, Yang S, Li N, Xu Q, Li H, Wang L, He J, Jiang J, Lu J (2016a) A versatile and cost-effective reduced graphene oxide-crosslinked polyurethane sponge for highly effective wastewater treatment. RSC Adv 6:38350–38355

Zhu T, Teng K, Shi J, Chen L, Xu Z (2016b) A facile assembly of 3D robust double network graphene/polyacrylamide architectures via γ-ray irradiation. Compos Sci Technol 123:276–285

Zhu Y, Zheng Y, Wang F, Wang A (2016c) Fabrication of magnetic macroporous chitosan-g-poly (acrylic acid) hydrogel for removal of Cd2+ and Pb2+. Int J Biol Macromol 93:483–492

Zhuang Y-T, Zhang X, Wang D-H, Yu Y-L, Wang J-H (2018) Three-dimensional molybdenum disulfide/graphene hydrogel with tunable heterointerfaces for high selective hg(II) scavenging. J Colloid Interface Sci 514:715–722

Zou J-P, Liu H-L, Luo J, Xing Q-J, Du H-M, Jiang X-H, Luo X-B, Luo S-L, Suib SL (2016) Three-dimensional reduced graphene oxide coupled with Mn3O4 for highly efficient removal of Sb(III) and Sb(V) from water. ACS Appl Mater Interfaces 8:18140–18149